ADDIS ABABA UNIVERSITY

SCHOOL OF EARTH SCIENCES

INTEGRATED GEOPHYSICAL METHODS FOR INVESTIGATIONS OF THE AYAT REAL ESTATE FOUNDATION: AN IMPLICATION FOR ENGINEERING WORK SUITABLITY, NORTHEASTERN ADDIS ABABA

BY

TEWODROS MISGANAW

A THESIS SUBMITTED TO THE SCHOOL OF GRADUATE STUDIES OF ADDIS ABABA UNIVERSITY IN PARTIAL FULFILMENT OF THE REQUIREMENT FOR THE DEGREE OF MASTER OF SCIENCE IN EXPLORATION GEOPHYSICS

AUGUST, 2020

ADDIS ABABA, ETHIOPIA

ADDIS ABABA UNIVERSITY

COLLEGE OF NATURAL AND COMPUTATIONAL SCIENCES

INTEGRATED GEOPHYSICAL METHODS FOR INVESTIGATIONS OF THE AYAT REAL ESTATE FOUNDATION: AN IMPLICATION FOR ENGINEERING WORK SUITABILITY, NORTHEASTERN ADDIS ABABA

BY

TEWODROS MISGANAW

SCHOOL OF EARTH SCIENCES

A THESIS SUBMITTED TO THE SCHOOL OF GRADUATE STUDIES OF ADDISABABA UNIVERSITY IN PARTIAL FULFILMENT OF THE REQUIREMENT FOR THE DEGREE OF MASTER OF SCIENCE IN EXPLORATION GEOPHYSICS

AUGUST, 2020

ADDIS ABABA, ETHIOPIA

Addis Ababa University

School of Graduate Studies

This is to certify that the thesis prepared by Tewodros Misganaw, entitled: Integrated Geophysical Methods for the Ayat Real Estate Foundation Investigations: An Implication for Engineering Work Suitability, northeastern Addis Ababa and submitted in partial fulfillment of the requirements for the Degree of Master of Science (Exploration Geophysics) complies with the regulations of the University and meets the accepted standards with respect to originality and quality.

Name of the candidate: Tewodros Misganaw Signature _____ Date_____

Approved by the Examining Committee:

Advisor: Prof. Tigistu Haile Signature _____ Date _____

Examiner: Dr. Abera Alemu Signature _____ Date _____

Dr. Zemenu Geremew Signature _____ Date _____

Dr. Bayisa Regassa _____

School Chairman or Graduate Committee Coordinator

Abstract

An integrated geophysical investigation was carried out at a site near Yeka-Ayat condominium and just in area about the middle of Ayat square and Tafo square, northeastern Addis Ababa, Ethiopia. The principal objective of this research is to map the subsurface geology of the site and discuss its suitability for the construction of large infrastructure. The method employed are the electrical resistivity tomography Vertical Electrical Sounding (VES) and Seismic refraction. Four VES points distributed along one profile line, four dipole-dipole survey lines spread and seismic survey on two profile lines were conducted to characterize the foundation materials within the study site. Qualitative and quantitative interpretations of the acquired data were made by comparing the results with borehole log data available from nearby areas. The results have revealed that the subsurface geology consists of three to four distinct units that reflect different physical properties (resistivity and seismic wave velocity). The upper most layer is characterized by low resistivity (3.03-25Ω-m) and low P-wave velocity (<0.42km/s) are associated with the response of the upper black cotton soil, composed of highly plastic clay and silty clay materials. The thickness of this layer is found to vary from 1.6m to 5.7m. Underlying the top layer, is a relatively thick (depth variation between 1.6m-12.4m) and its resistivity varying from 30-42Ω-m and P-wave velocity(<1.79) this response is due to light gray, medium to highly plastic clay, which is found inclined from north to the southern direction of the study area. In order to the result of 2D resistivity models, geo-electric section of VES and seismic velocity model of the third layers are the response of slight to moderate ignimbrite. It represents the bedrock of undulating morphology in the study area and is characterized by increment in depth (varying from 12.3m to 37.6m) in a direction from north to south of the study area. Its resistivity is varies from 38 to 65Ω-m and P-wave velocity less than 2.4km/s. Whereas the bottom layer mapped with the survey is a fine and slightly weathered bed rock, clearly observed under the first 20-60m distances of the study area. Its depth is found to vary from north to south direction and its resistivity from 86 to 206Ω-m. From the result of ERT profiles and VES profile around 50m and 70m distances there is hidden structure/fracture in the subsurface, which is oriented from NW to SE. Which is similar to seismic refraction around 20m and 40m distance of the profile south to north direction. Generally, the study result shows that the entire study area is characterized by low resistivity, which is less 206Ω-m and this resistivity is a response of a mostly saturated layer with those higher resistivity to be responses of weathered and fractured formations of low moisture content. Areas of potential weakness have been mapped. Utilization of the site for, development of engineering structures around this site requires proper measures, including proper drainages, compaction, stabilization, removing and backfilling of the top

soil and filling by other well graded material that enable to make the structures with stand soil expansion and the impacts from natural geo-hazard events.

Key words: Site characterization, Rift margin, Dipole-Dipole tomography, Seismic refraction, Seismic wave velocity, Ethiopia

Acknowledgements

Above all I would like to thank the Almighty God for keeping my health and help to do my day to day activities.

Firstly, my heartfelt thanks goes to my advisor Prof. Tigistu Haile for his help during my field work, fatherly approach, encouragement, crucial comments and sound suggestions that he provided throughout my research work. To speak frankly, I haven't words to express his support and fatherly advice not only the subject matter but also for my future career.

It is my pleasure to also thank Prof. Tilahun Mommo for his help in calibrating the seismic device and Dr. Addis Eshetu for his limitless help in seismic data acquisition during field work and friendly approach.

I am also thankful to the Ayat real estate pls. for allowed to me the site and Addis Ababa Housing Agency where I got the direct geotechnical data and lithological logs of the study area. I am also thankful to the school of Earth Sciences, Addis Ababa University for their finance and equipment support that was extended for the present research work.

Last but not the least: - I am thankful you to all my families and friends for their support and encouragement during the period of this thesis work.

Table of content

Content Page

Abstract....iv

Acknowledgements....vi

List of Figures....x

List of Tables....xi

List of Acronyms....xii

CHAPTER ONE: INTRODUCTION....1

1.1. General....1

1.2. Description of the study area....3

1.2.1. Location....3

1.2.2. Topography of the study area....5

1.3. Literature Review....6

1.4. Problem Statement....7

1.5 Objective of the research work....7

1.5.1 General objective....7

1.5.2 Specific Objectives....7

1.6 Methodology....8

1.7 Structure of thesis paper....9

1.8 Limitations of the study....9

CHAPTER TWO: GEOLOGY, SEISMICITY AND HYDROGEOLOGY OF THE STUDY AREA....10

2.1. Geology of Study Area and its Surrounding....10

2.1.1. Entoto Silicic Volcanics....11

2.1.2. Addis Ababa Basalt....12

2.1.3 Nazareth Group....12

2.1.4 Bofa Basalts....13

2.1.5 Wechacha trachyte....13

2.2 Seismological setting....14

2.3 Hydrological setting....15

CHAPTER THREE: THEORETICAL BACKGROUND OF METHODS OF INVESTIGATION....17

3.1 Introduction 17

3.2. The Electric Resistivity Method 17

3.2.1. Basic theory and principles 17

3.2.2. The relationship between geology and Electrical resistivity 20

3.2.3. Useable techniques of electrical resistivity 21

3.2.3.1. Vertical Electrical Sounding (VES) 21

3.2.3.2. Interpretation of Vertical Electrical Sounding 22

3.2.3.3. 2D Electrical Resistivity Tomography 25

3.3 Fundamental Principle of Seismic Method 30

3.3.1 The relationship between Geology and Seismic Velocity 35

CHAPTER FOUR: FIELD DATA ACQUISITION, PROCESSING AND PRESENTATION 37

4.1. Survey layout and profile selection 37

4.2 Electrical resistivity 37

4.2.1 Data acquisition and instrumentation 37

4.2.1.1 Vertical Electrical Sounding (VES) 37

4.2.2 Data processing and presentation 39

4.2.2.1. Vertical electrical sounding 39

4.2.2.1 Electrical Resistivity Tomography 41

4.3. Seismic Refraction survey 42

4.3.1 Data acquisition and instrumentation 42

4.3.2 Processing and presentation of seismic data 43

CHAPTER FIVE: RESULT, DISCUSSION AND INTERPRETATION 45

5.1 Introduction 45

5.2 Electrical resistivity survey 45

5.2.1. Vertical Electrical Sounding (VES) 45

5.2.1 Electrical Resistivity Tomography (ERT) 48

5.2.1.1 ERT (along Profile 1) 48

5.2.1.2 ERT (along Profile 2) 49

5.2.1.3 ERT (along Profile 3) 50

5.2.1.4 ERT (along Profile 4) 51

5.2.3 Combination of the 2D electrical resistivity tomography profiles 52

5.3 Seismic refraction survey 53

5.3.1 Velocity model for profile_1 53

5.3.2 Velocity model for Profile_2 54

5.4. Integrated geophysical and geological data analysis 54
5.4.1 Analysis of 2D ERT models and VES geo-electrical sections 54
5.4.1.1 ERT-Profiles-2 and VES profile 55
5.4.2 Analysis of seismic refraction Profile-2 and VES geo-electrical section 55
CHAPTER SIX: CONCLUSIONS AND RECOMMENDATIONS 57
6.1 General 57
6.2 Conclusions 57
6.3 Recommendations 58
References 60
Appendix 65

List of Figures

Figure1. 1: City of Addis Ababa and the location of the study area. *4*
Figure1. 2: DEM showing physiographic map of Addis and the overall topography of study area. *5*
Figure1. 3: Partial view of study area. *6*
Figure1. 4: Flow chart of methodological approach. *8*
Figure 2. 1: Geological map of Addis Ababa (after Ethiopia Geological Survey, 2017). *11*
Figure2. 2: The major Earthquake-causative tectonic features Ethiopia (Mulugeta Dadi, 2015). *15*
Figure3. 1: Arrangement of electrodes to flow electric current through the Earth *18*
Figure3. 2: The resistivity of rocks, soils and minerals (Loke, 2004) *21*
Figure3. 3: The Schlumberger electrode arrangement. *22*
Figure3. 4: Two-layer master curves for Schlumberger array (Shendi, 2008). *24*
Figure3. 5: The four types of three-layer VES curves; the three sample curves for each of the four types represent values of d2/d1= 1/3, 1 and 3 respectively (Shendi, 2008). *25*
Figure3. 6: The Dipole-Dipole electrode setup. *26*
Figure3. 7: Common arrays used in resistivity surveys and their geometric factors (Loke, 2000). *27*
Figure3. 8: Electrode array of dipole-dipole profiling survey with depth information included. *28*
Figure3. 9: propagation of Seismic refraction energy through subsurface *31*
Figure3. 10: seismic refraction principles a) Snell's Law and refraction of ray transmitted across boundary between two media with different velocities, b) Travel-Time graph for two layer surface, c) A two layer horizontal stratified substratum (Redpath, 1973). *32*
Figure3. 11: multi-layered horizontal stratified substratum *34*
Figure 4. 1: The geophysical survey lines. *38*
Figure4. 2: The electrical resistivity surveying instruments utilized in this study. *39*
Figure4. 3 Examples of individual VES interpreted curves of VES1 and VES4. ..... *40*
Figure4. 4 Measured, calculated and inverse 2D resistivity model of ERT Profile-4. ..... *41*
Figure4. 5: Seismic refraction survey instruments. *42*
Figure4. 6: a) Wave form data and picked first break (red vertical lines) at the middle shot of Profile-1 and, b) time –term velocity model for the same profile. *44*
Figure 5. 1: The apparent resistivity pseudo-section along VES Profile. *46*
Figure 5. 2: Geo-electric section of the VES profile, Ayat Zone 8, Northeastern Addis Ababa. *47*
Figure 5. 3: 2D resistivity model section along ERT-1. ..... *49*
Figure 5. 4: 2D resistivity model section along ERT-2. ..... *50*
Figure 5. 5: 2D resistivity model section along ERT-3. ..... *50*
Figure 5. 6: 2D resistivity model section along ERT-4. ..... *51*
Figure 5. 7: Stacked apparent resistivity map of the ERT data. *52*
Figure 5. 8: Velocity model along Profile_1. ..... *53*
Figure 5. 9: Velocity model along seismic Profile-2. ..... *54*
Figure 5. 10: Correlation of the ERT result of Profile-2 versus geo-electrical section of VES profile. *55*

Figure 5. 11: Correlation of the seismic refraction Profile-2 versus geo-electrical section of the VES profile.....56

List of Tables

Table2. 1: previously occurred earthquakes in Addis Ababa (after Gouin, 1979 and IGSSA).....14

Table3. 1: The median depth of investigation (z e) for the different arrays. L is the total length of the array. Note identical values of z e/a for the Wenner-Schlumberger and pole-dipole arrays (Loke, 1999) 29

Table3. 2: Compressional wave velocities in Earth materials (Kearey et al., 2002).....35

Table4. 1: Seismic refraction data acquisition and processing summary.....43

List of Acronyms

AFMAG	Audio-Frequency Magnetic
BBC	British Broadcast Corporation
EM	Electromagnetic
ERT	Electrical Resistivity Tomography
ETV	Ethiopia Television
HERT	High-resolution Electrical Resistivity Tomography
IGSSA	Institute of Geophysics, Space science and Astronomy
IP	Induced Polarization
MER	Main Ethiopian Rift
NE	Northeast
N	North
S	South
SP	Self Potential
SW	Southwest
RMS	Root Mean Square
VES	Vertical Electrical sounding
2D	Two Dimensional
3D	Three Dimensional

CHAPTER ONE
INTRODUCTION

1.1. General

Civil engineering structures like buildings, bridges, highway, tunnels, dams, large towers, etc. are founded below or on the surface of the Earth. For their stability, suitable foundation of soil and rock are required (Laskar, 2012). Foundation is an integral part of a structure that transmits the weight of the structure to the soil underneath it (Oyediran et al., 2018). The classic foundation types usable in the erection of civil engineering structures include both shallow and deep footing. The appropriateness of these foundation types to building infrastructure, including low- and high-rising buildings largely depend on the subsoil geotechnical and geophysical parameters characterizing the varying lithological layers at depth. Thus, the potential of geophysical and geotechnical techniques in mapping and evaluating subsurface formations and physical/engineering properties of the foundation materials is an important exercise. Foundation conditions are investigated with a view towards attaining a future design of good foundations that can address the incessant structural tragedies peculiar to engineering infrastructural development (Olayanju et al., 2017). To this end, the physical and chemical property of soil and rocks must be properly conducted for the stability of foundation. If the physical property and chemical property of soils and rocks are not studied properly the performance of the structures may be affected by natural or human made disasters like earthquakes (e.g., the Karakore and Hosanna earthquakes (ETV News (2016)), BBC News 2015), wind, floods, etc.

The main purpose in the study of properties of soils and rocks in relation to their suitability for large foundation is to lay down certain principles, theories and procedures for the design of a safe and sound structure. According to (Oyediran et al., 2018), when failure of any structural element occurs, many factors are often responsible for it which includes improper foundation investigation, poor building design, poor materials and inexperience of the handler as the case maybe. And also as the Bible says, “Therefore whosever heareth these my words, and doeth them, shall be likened to a wise man who built his house upon a rock, and the rain fell, and the floods came, and the winds blew, and they beat upon that house, and it fell not, for it was founded on a rock” (Challoner, 1847).

In Ethiopia, diversified geological, tectonic, climatic and geomorphological situations exist and prominent natural events of geo-hazards like landslides, earthquakes, ground collapses, sinking and the like are also manifested making the country subjected to the effects of the combination of these factors. Specifically, in Addis Ababa, the geology is covered by different volcanic rocks, the city is near the Main Ethiopian Rift

(MER), the existence of Filwuha fault at the middle of the city by itself and the existence of thick black cotton soil in the majority areas of the city potentially aggravate the occurrence of geo-hazards which eventually lead to infrastructural devastation, property loss and loss of live.

Impending urbanization is rapidly increasing the population Addis Ababa. Hence, massive constructions are currently undertaken by private and government owners to suite different purposes. Amongst the, massive residential house constructions are undergoing to solve housing problem and modernize the city. However, most of the constructions are carried out with limited geotechnical investigations that incorporate scarce borehole data with insufficient depth to adequately understand the subsurface and also lacking continuous coverage of the construction sites. Therefore, in a city like Addis Ababa, where a radical change is manifested in the form of rapid population growth, infrastructural development, industrialization and modern urbanization, the existence of proper site investigation is important to construct the building foundation safely.

Examination of the engineering geological properties of soils and rocks for geotechnical investigations require borings and/or sampling in a close-order grid. These investigations provide information on the physical or mechanical and chemical properties of rocks and soils that are relevant to the design of a foundation for proposed structures. Other important aspects to be obtained from such studies are the depth of the building foundations and the presence of any irregularities in the subsurface revealed during excavation. Yet, one commonly accepts geotechnical data from a limited number of data points to characterize large areas and complex geologic settings (Benson, 1993). The result of geotechnical data will obtain from the limited number of tests and due to this, geotechnical data cannot represent the wide area due to the possibility of existence of inhomogeneity of the subsurface of Earth and it may lose the required complete information about the site condition. Therefore, to obtain a complete picture of the site conditions and minimize the high cost requirements of large number of geotechnical boreholes, measurements taken over denser spacing and in a continuous manner (using geophysical techniques) are more useful and represent the real conditions than direct samplings at selected points (geotechnical investigation) over the area of study.

Geophysical techniques can be taken with denser measurement spacing than direct sampling and involve much less costs, and hence, are potentially useful in characterizing building sites with adequate accuracy when large sites are to be studied (Tigistu Haile et al., 2014). Geophysical techniques can further provide wide-area method for subsurface characterization and obtain information regarding relevant material property (Oyediran et al., 2018), such as soil properties, bedrock depth and its topography below

unconsolidated material, rock types, layer boundaries, water table depth and presence of weak zones and expansive clays (Aubert (1984) as cited in Tigistu Haile et al., (2014).

For a better characterization of the subsurface beneath an area selected for foundation, geophysical and geotechnical results can be combined to discover the property of the subsurface, because both of them focus on the behavior and performance of soils and rocks in the design and construction of civil, environmental and mining engineering structures. Soupios et al., (2007), has shown that geophysical methods when used in coordination with geotechnical investigations are able to provide solutions to these problems, and may even disclose several types of structures that typical geotechnical methods like drills/ boreholes/, or field investigation, might fail to detect.

In this study, a combination of surface geophysical investigation techniques such as 2-D electrical resistivity imaging, Vertical Electrical Sounding (VES) and seismic refraction survey are used in coordination with available geotechnical data are used to obtain detailed picture of the underground conditions without the requirement of much costly large number of digging and to determine its suitability for building foundations for Ayat real estate site in Zone 8, on the northeastern side of Addis Ababa.

1.2. Description of the study area

1.2.1. Location

The study area is located in the central Ethiopian highlands and close to the western edge of the Main Ethiopian Rift (MER). More specifically, the site is situated on northeastern side of Addis Ababa, around YekaAyat condominium construction site at the edge of a main asphalt road going to Lege Tafo and Legedadi areas. It is geographically bounded between around 9° 2'7"N and 9° 2'15"N latitude and38°52'30"E and 38°52'40"E longitude as shown in Figure 1.1.

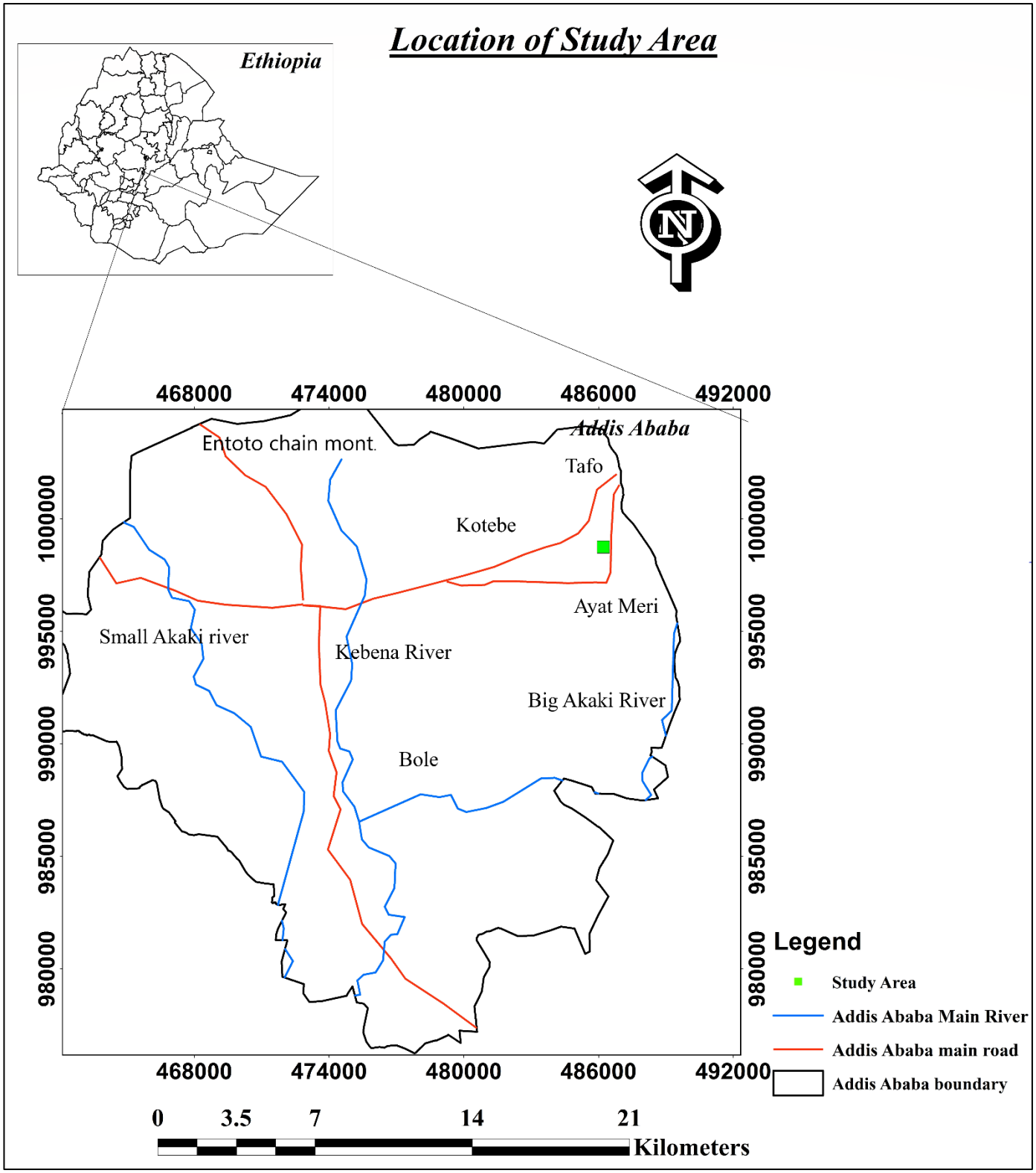

Figure1. 1: City of Addis Ababa and the location of the study area.

1.2.2. Topography of the study area

Physiographically, the city of Addis Ababa is situated at a south facing slope of the Ethiopian Rift Valley. The volcanic mountains surrounding the city include Entoto Chain Mountain in the north, Wechecha range in the west, and Mount Furi in southwest and further south east of the city lies Mount Yerer (Figure 1.2). The elevation is general decreases in the north to south direction follow which. In the drainage of the city also follows from north the south direction (Tesfaye Asresahagne et al., 2016). One of the rivers draining the city, the Big Akaki River exists at about 1.5km from the study area in the southeast direction. The study area topography is slopping from northwest to southeast direction shown on the DEM plot given in Figure (1.2). The studied area has minimum and maximum elevation respectively ranging from 2436m to 2449 m above mean sea level. Around the study area, there are the Yeka-Ayat condominium buildings which cover large area constructed by government organizations. The general field setting and partial view of the studied area is shown in Figure 1.3

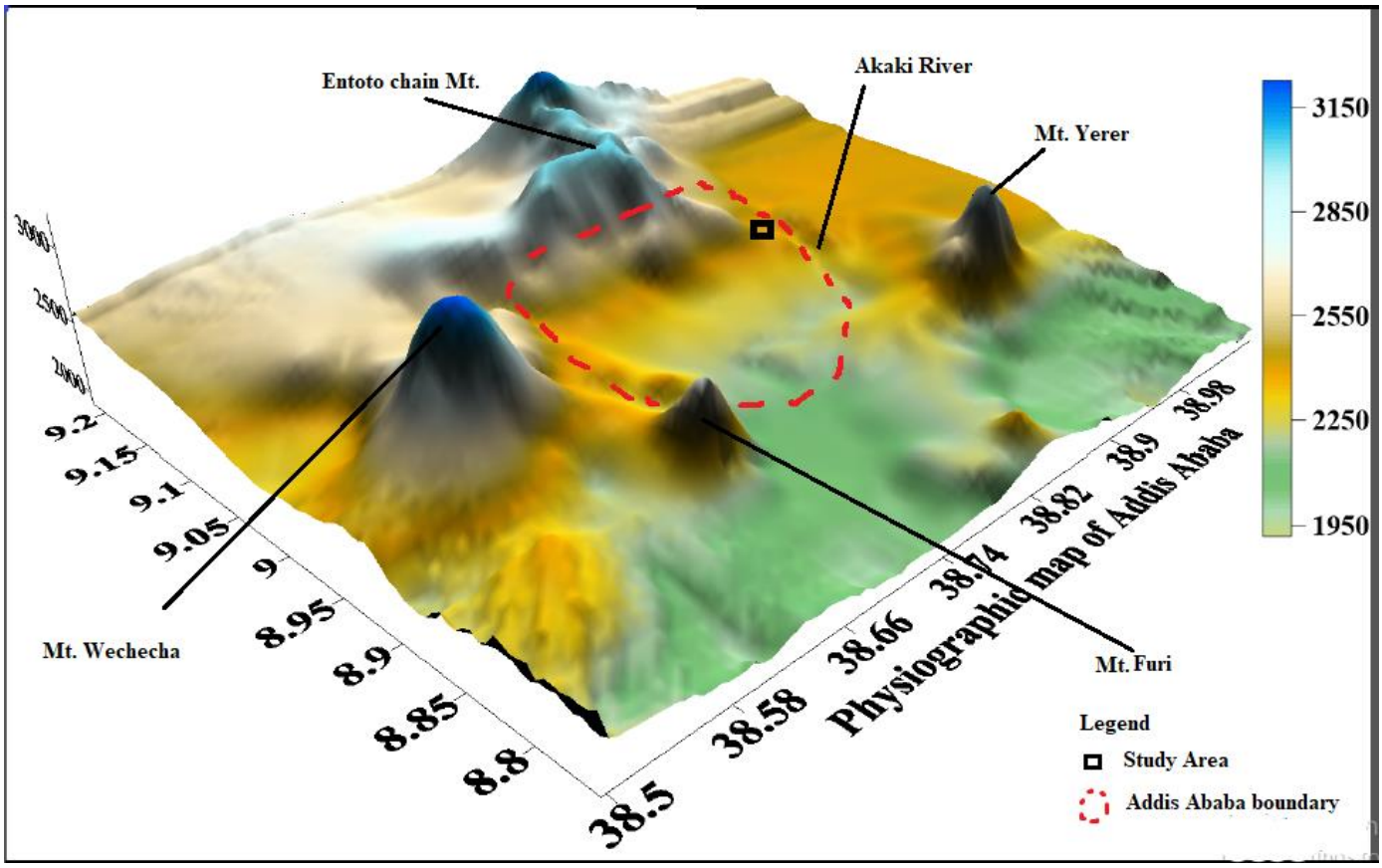

Figure1. 2: DEM showing physiographic map of Addis and the overall topography of study area.

Figure1. 3: Partial view of study area.

1.3. Literature Review

Several researchers have been involved in geological site investigation of Addis Ababa city using geophysical and geotechnical techniques individually as well as cooperatively. Tilahun Mammo (2005), Atalay Ayele(2005), Hailemariam Siyoum and Tigistu Hiale (2011), Belete Getahun (2018) made site investigation for construction over various locations around Addis Ababa; these include sites around Addis Ababa Science and Technology University, Akaki Kality sub city, Kebena, Kechene and Saris Abo areas to mention just a few. These works used geophysical techniques (electrical resistivity, seismic refraction and magnetics) for field work and geotechnical method as secondary data cooperatively to characterize their respective study sites. In addition to these, Tamiru Alemayehu (2001), Tenalem Ayenew et al., (2008), Engida Zemedagegnehu (2001), Tigistu Haile (2012), Molla Demlie et al., (2007), Eyasu Leta, (2014) used geophysical and geotechnical methods to study the quantity and quality of groundwater in Addis Ababa area. According to their studies, the groundwater of Addis Ababa flows in a north to south direction of the city. The rocks and material on the northern direction of Addis Ababa showed low porosity, high bulk density, good comprehensive strength and very low water absorption. The depth of the groundwater in general is found to increase in the south direction which is the Akaki catchment drainage and flow direction. There are also relatively deeper groundwater areas of more than 120 meters depending on the topography of the area and the shallow groundwater are found to be more polluted. Other researchers, Tesfaye Asresahagne et al., (2016), Haile Selassie Girmay et al.,(1989), Aseged Getahun, (2007), Selamawit Tadesse, (2017) and Medhanit Akalu (2017), studied the Addis Ababa city geology and used geotechnical methods to characterize the soil and rocks and examine their suitability for construction. As they reported, the geology of the city of Addis Ababa and its surroundings is dominantly of volcanic rocks comprising of both acidic and basic

compositions such as tuff, rhyolite, ignimbrite, trachyte, and basalt. Specially, Tesfaye Asresahagne et al., (2016) described the geology of Ayat-Meri area, an area close to the area of study of the present work, as having the dominant geology of the area being of ignimbrites which cover the flat, large part of farmlands overlying the tuff unit.

1.4. Problem Statement

All civil engineering structures are constructed either in soil or rock, but all soil and rocks may not be suitable for engineering construction. Therefore, before construction of civil engineering structures, there is a need for sufficient information about the geophysical and geology properties of soil, engineering properties of the soil and rocks, geological structures and the groundwater saturation of the site. In Ethiopia mostly geotechnical investigation of a site is conducted by limited number of boreholes and trenches. Such investigation is obviously not enough to represent large area, because the internal surface of Earth is completely inhomogeneous. Addis Ababa being situated on the margin of the active East African Rift System which the Main Ethiopian Rift (MER) (Figure 2.2) makes a part the importance of a study where adequate continuous data covering the area are required to characterize the site (Tilahun Mammo, 2005). The existence of potential active faults (e.g. the Filwoha fault running parallel to MER and related to it Tamiru Alemayehu, 2001), failure surfaces, fractures, underground cavities and ancient buildings and human activity remains which are relevant to design building foundation are difficult to detect by these sparsely placed geotechnical data inputs.

Geophysical methods can help to solve the above problems and are capable of producing better investigation of the subsurface in a continuous manner and in obtaining additional inputs for characterizing the engineering properties of soil and rocks of a large surface area of Earth by using measurements with denser spacing.

1.5 Objective of the research work

1.5.1 General objective

The main objective of this research is to characterize the Ayat Real Estate, Zone 8 building site in the northeastern part of Addis Ababa its suitability for engineering work based on the result of geophysical site investigation techniques.

1.5.2 Specific Objectives

The Specific objectives of this research are:

- To determine the depth and thickness of the geological strata and their potential influence on the building foundation,
- To determine depth to the bedrock,

- To map the morphology of the bedrock,
- To characterize the soils and rocks of the site in terms of their engineering geological properties and their influence on the building foundation,
- To determine the existence, depth and thickness of groundwater saturation zone (if it exists at shallow depth).
- To detect lateral and vertical changes in rock characteristics and locate local anomalous geological conditions, lithological contacts and structures that could be detrimental to the building foundations.

1.6 Methodology

The methodology used in this research is based on the listed general and specific objectives in section 1.5. Geophysical method of investigation were employed in which the electrical resistivity imaging and VES were respectively used. Primary data were collected along the profiles by using listed geophysical methods. The existing borehole data collected from Adds Ababa House Corporation were used for this research. The generalized Flow chart of methodological approach is described in Figure1.3

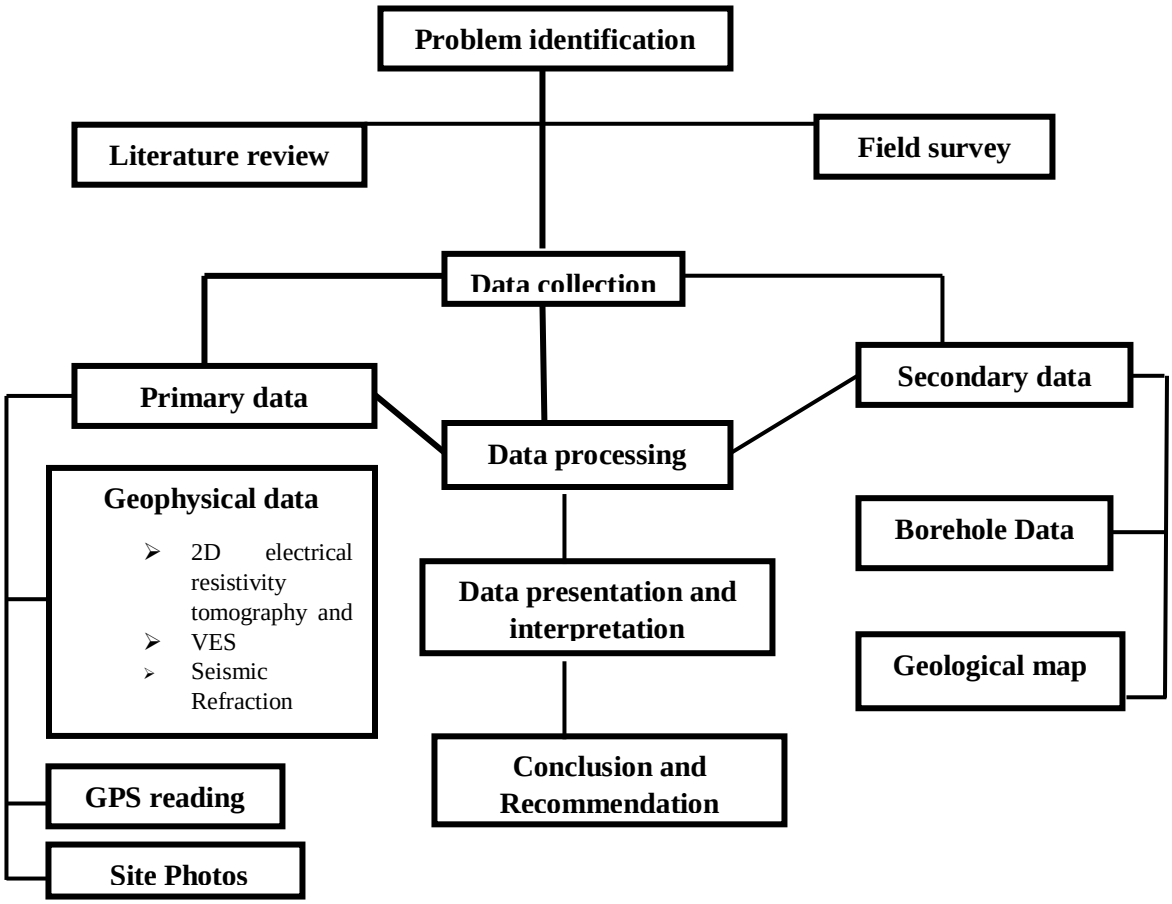

Figure1. 4: Flow chart of methodological approach.

1.7 Structure of thesis paper

This thesis paper is organized in to six Chapters. The first Chapter includes general introduction of the study, describes the specific location and topography of the study area, statement of the problem, previous works in the study area and its surroundings and methodologies used in of the present study. The second Chapter is concerned mostly with the work of previous researchers that includes geology, hydrogeology and seismicity of the study area and its surrounding. Chapter three covers the theoretical background for the geophysical methods employed in this study. Chapter four describes the complete survey procedure, data acquisition, data processing, and presentation of the different results. In this chapter, discussion on how the data was collected (number, length and orientation of the profiles and number of electrodes and employed and the data volume), the type of software used and how the software are employed to analyze the geophysical data. Chapter five covers integrated results and interpretations of different geophysical methods data which is analyzed in chapter four. The last chapter contains conclusions and recommendations of the research work.

1.8 Limitations of the study

Maximum effort has been made to effectively carry out this thesis work through the allocated time and financial resources. Well planned and proper field survey has been carried out in different seasons to acquire reliable geological information about the vertical and horizontal stratification of construction site. However, some situations render the field survey as well as the final interpretation of this study. Some of the major limitations encountered are stated as follows:

a. As the study area is located near the Yeka-Ayat condominium site, it was covered by deposited soil which has been excavated from the condominium site and deposited as wasted material on the area of study, the loose material makes it difficult to secure good connection for geophones and energy transmission.
b. The area of the study is a confined and fenced compound and not large enough to do the large electrode spacing required for deeper investigation and to do survey on a number of VES profiles.
c. Absence of well-documented lithological log data within this specific site has made it difficult to make a refined detailed geophysical data interpretation.

CHAPTER TWO

GEOLOGY, SEISMICITY AND HYDROGEOLOGY OF THE STUDY AREA

2.1. Geology of Study Area and its Surrounding

The city of Addis Ababa is situated on the margin of the active East African Rift System which the Main Ethiopian Rift makes a part. As such the geology and structural features within and around the city are influenced by all the processes related to the formation and subsequent growth of the Rift System (Tilahun Mammo, 2005).

Addis Ababa is surrounded by volcanic mountains that include Entoto Chain Mountain in the North, Wechacha range in the west and Mount Furi in the southwest, and Mount Yerer in the southeast (Tesfaye Asresahagne et al., 2016). There is a general decrease in elevation from north to south direction (Figure 1.2). The geology of Addis Ababa has been reported to be dominantly of volcanic rocks comprised of both acidic and basic compositions such as tuff, rhyolite, ignimbrites, trachyte (Figure 2.1; Karstaedt and Wondafrash, 1986 as cited in Tesfaye Asresahagne et al., 2016).

At a local scale, the study area is located around 1.5 Km due north from Ayat condominium construction zone 5 and around 2km from Meri. The dominant geology of the Meri area is ignimbrite which covers the large part of farmlands overlying the tuff unit. The tuff unit occurs in sloppy areas and subdued topographies, which at places form small cliffs as a result of intermediate compaction. The rock in this area is most preferred for wall cladding and other decorative purposes and is under exploitation as observed during field excursion in the area. The unit has intermediate compaction perhaps less than that of the ignimbrite and more than ordinary tuff (Tesfaye Asresahagne et al., 2016).

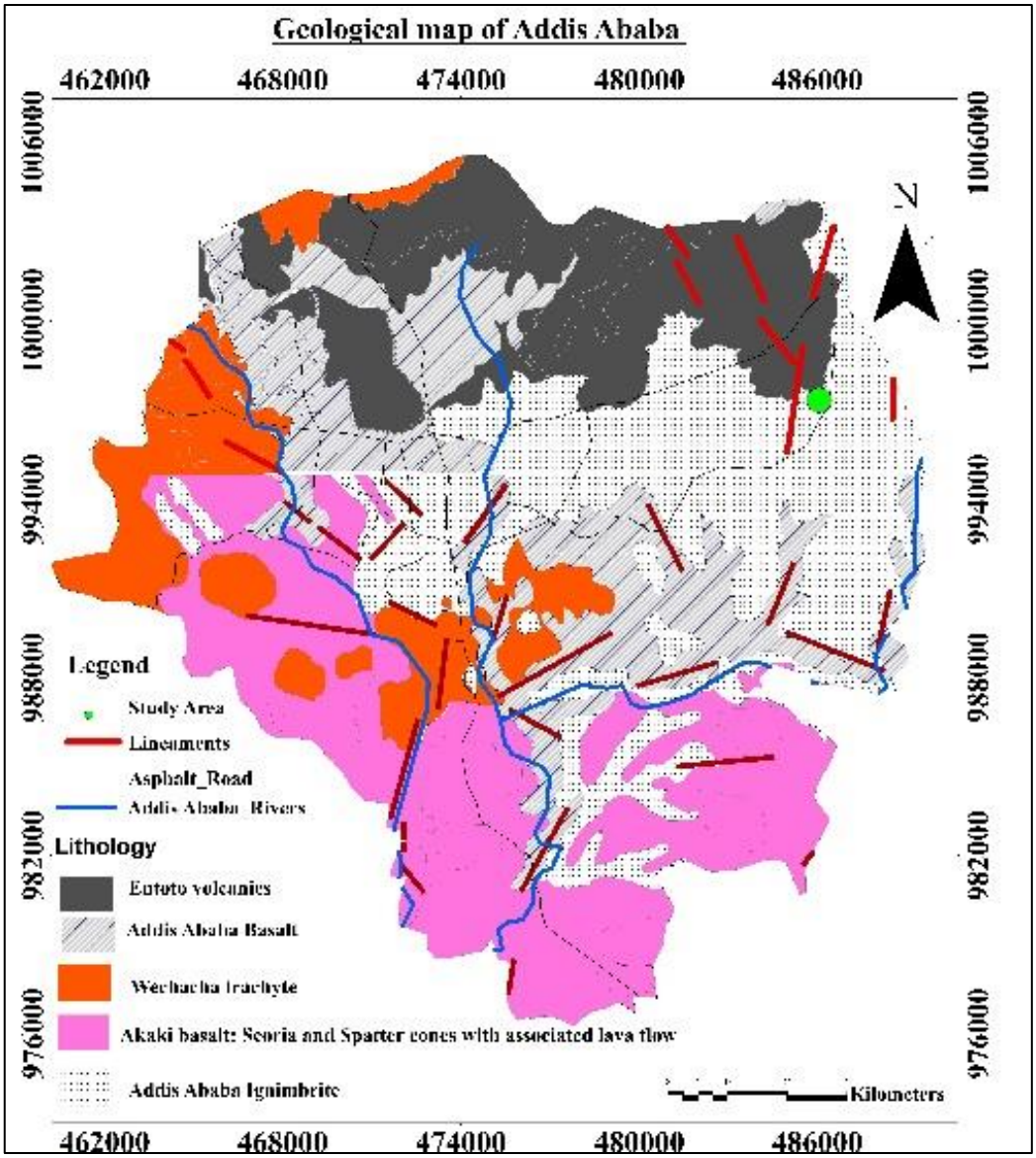

Figure 2. 1: Geological map of Addis Ababa (after Ethiopia Geological Survey, 2017).

2.1.1. Entoto Silicic Volcanics

The Entoto Silicic volcanic are unconformable overlain by Addis Ababa basalt on the foothill of Entoto Mountain which straddles the northern side of the City. These early Miocene aged silicic volcanic units could represent localized terminal episodes to massive Oligocene fissure-basalt activity in the Addis Ababa region (Morton et al., 1979). The thickness of the flow becomes maximum on top of Entoto ridge and thin both towards the plateau and the plain east of Addis Ababa. The Entoto silicics are composed of rhyolite and trachyte units with minor amount of welded tuff and obsidian (Haile Sellasie Girmay et al., 1989).

2.1.2. Addis Ababa Basalt

The basalts of Addis Ababa, Pliocene in age, are described as the youngest porphyritic olivine basalts, the intermediate age porphyritic feldspar basalts and the oldest aphanite basalts. Of these basalts the most diffuse are the olivine basalts (6.9 and 7.3 Ma) that cover a large area starting from just north of the Legehar railway station up to the extreme north of the city to the foot of the Entoto hill (Tilahun Mammo, 2005). The maximum thickness of the unit exceeds 130 meters and the outcrop is found exposed at Ketchene stream. Olivine porphyritic basalts outcrop in the central part of the town that includes Mercato, Teklehaymanot and Sidist Kilo. The distribution of plagioclase porphyritic basalt is almost the same as that of the olivine porphyritic basalt. It outcrops in an area, which includes Sidist Kilo, General Winget School and French Embassy (Haile Selassie Girmay et al., 1989).

2.1.3 Nazareth Group

The units identified in this group are denoted as Lower Welded Tuff, Aphanitic basalt and Upper Welded Tuff. The group is underlain by the Addis Ababa basalt and are overlain by Bofa basalts. The rocks outcrop mainly south of Filwoha fault and extend towards Nazareth (Tamru Alemayehu et al., 2006).

The Lower Welded Tuff unit is the rock that outcrops as small discontinuous body in Filwoha, western parts of Addis Ababa and Sululta. Generally, it is overlain by the aphanitic basalt and underlain by the olivine and plagioclase porphyritic basalt. The age of this rock unit, as dated by Morton et al. (1979), and as cited in Tamru Alemayehu et al., (2006), at Addis Ababa and Sululta is 5.1 and 5.4 million years, respectively. This age overlap with the period of the activity of Wachecha trachyte volcanoes, dated 4.6 million years. Wachecha is located about 15km west of Addis Ababa and is probably the sources of the Lower welded tuff at both localities (Morton et al., 1979).

The Upper Welded Tuff rock unit outcrops all over the southern part of the town including Bole, Nefas Silk and Railway station areas; nevertheless it is also present in the central and northern parts of the town. It is gray colored, vertically and horizontally jointed and composed of sandine, an orthoclase, rebecite, quartz, pumice and unidentified volcanic fragments (Haile Selassie Girmay et al., 1989).

The Aphanitic Basalt covers the southern part of the town, especially the areas of Bole International Airport and Lideta Airfield. The rock body shows vertical curved columnar jointing together with sub horizontal sheet jointing. Kaolin and lenses are present at the contact of this basalt with the younger ignimbrite. This gives an evidence for the hydrothermal alterations along a NE-SW fracture system, which may affects both the basalt and the Entoto trachyte.

The Young Trachyitic Flow rock is predominating in the south west part of the town, from Dama Hotel towards Furi and Repi along the hills and foothills of Hana Mariam and Tulu Dimtu. It is porphyritic with phenocrysts of plagioclase (albite-oligoclase) sandine, biotite within a ground mass of microlities of feldspar. Moreover, it is underlain by the tuff that covers the young ignimbrite and overlaying by alternating flows of plagioclase porphyritic basalt and rhyolite especially in the Repi hill. Its relation with the young olivine prophyrytic basalt is not clear as they outcrop in different parts of the areas; however, in a small outcrop nearby Aba Samuel Lake far south of the project area, the trachyte underlies the olivine porphyritic basalt (Tamru Alemayehu et al., 2006).

2.1.4 Bofa Basalts

Bofa Basalts outcrop southward from Akaki River where they appear in the form of boulders reaching a thickness of 10 meters. They are restricted in extent and dominant in the southeastern parts of the city. This rock unit is characterized by big vesicles that are filled by calcite. This basalt is underlain by the tuffs which cover the welded tuff (Tamru Alemayehu et al., 2006).

2.1.5 Wechacha trachyte

This unit is located in the western part of Addis Ababa. It forms about 18% of the total area and covers an area of about 553 sq.km. The unit mostly forms big mountains such as Furi, Wechecha and Yerer and found overlying the Repi basalt and the contact is marked by a thick paleosoil. But, in some localities it is covered by Quaternary Olivine-phyric basalt. It is an aphanitic to medium grained in texture with vesicular varieties mostly at its lower part. This trachyte and trachy basalt is light grey to dark grey often to greenish grey. Weathered surfaces of the unit show various colors. It has aphanitic to vesicular texture. At its lower part, it shows columnar jointing and is affected by two sets of joints. At some places it shows layering. Mostly the trachytes and the trachy basalts are found alternatively layered with the trachyte being dominant. The base of the unit is dominated by trachy basalt basaltic rock type. Thin section studies on samples from this unit show a composition of 20-60% plagioclase, 5-12% olivine minerals and 15-70% groundmass. The groundmass is made up of olivine, pyroxene, plagioclase and opaque minerals. The pyroxene and olivine minerals are weathered to form secondary minerals of augite and iddingsite. The rock shows poikilitic texture (Aseged Getahun, 2007).

2.2 Seismological setting

The city of Addis Ababa which is located at about N 9.02 and E 38.45 is near the western escarpment of the Ethiopian rift valley seismic source zone (Messele Haile, 2004) as shown in Figure 2.2. The city is extremely extended in areal coverage and there is a rapid growth through building constructions, population and infrastructures compared to the previous years. These building constructions and the increasing population may be the cause of additional load to the many infrastructures like roads and public amenities.

According to Gouin (1979), Addis Ababa has witnessed a number of earthquakes in 100 years of its existence, some in the list of the highest intensity earthquakes are the 1906 (Langano) and the 1961 (Kara Kore) earthquakes(Table 2.1). The only major earthquake sequence ever to shake Addis Ababa in living memory occurred from the June to September 1961 near Kara Kore with a main shock magnitude of 6.6 (Atalay Ayele, 2005).

Table2. 1: previously occurred earthquakes in Addis Ababa (after Gouin, 1979 and IGSSA)

Year	Earth quack magnitude	Epicenter distance from Addis Ababa	Location
1906	6.8	100km	Langano
1961	6.7	200km	Karakore-Majete
1979	4.1	22km	Akaki
1985	4.9	131km	Butajira
1985	4.7	120km	Debre Birhan
1993	5.0	92km	Nazereth
2009	5.0	172km	Ankober

The 1906 earthquake (more than 120 km away from Addis Ababa) occurred when the city was at its infancy with few population, few buildings and with no infrastructure laid down and hence no significant casualties were registered. But oscillation of suspended objects, wide spread cracking of roofs, doors and windows, spontaneous ringing of church bells as well as great panic in the city. However, with the 1961 Kara Kore earthquake, which is located about 200 km away from the city of Addis Ababa, relatively bigger damages were reported (Gouin, 1979). It was further noted that tremors were felt in the city for 2 weeks. It is also stated that the tremors were followed by a wave of rustling noises generated by the twisting of the corrugated iron roofing sheets covering most houses, some masonry structures cracked, partition walls in reinforced concrete frame buildings were dislocated by shearing motion, etc. Schools were closed for 3–4 days (Tilahun Mammo, 2005).

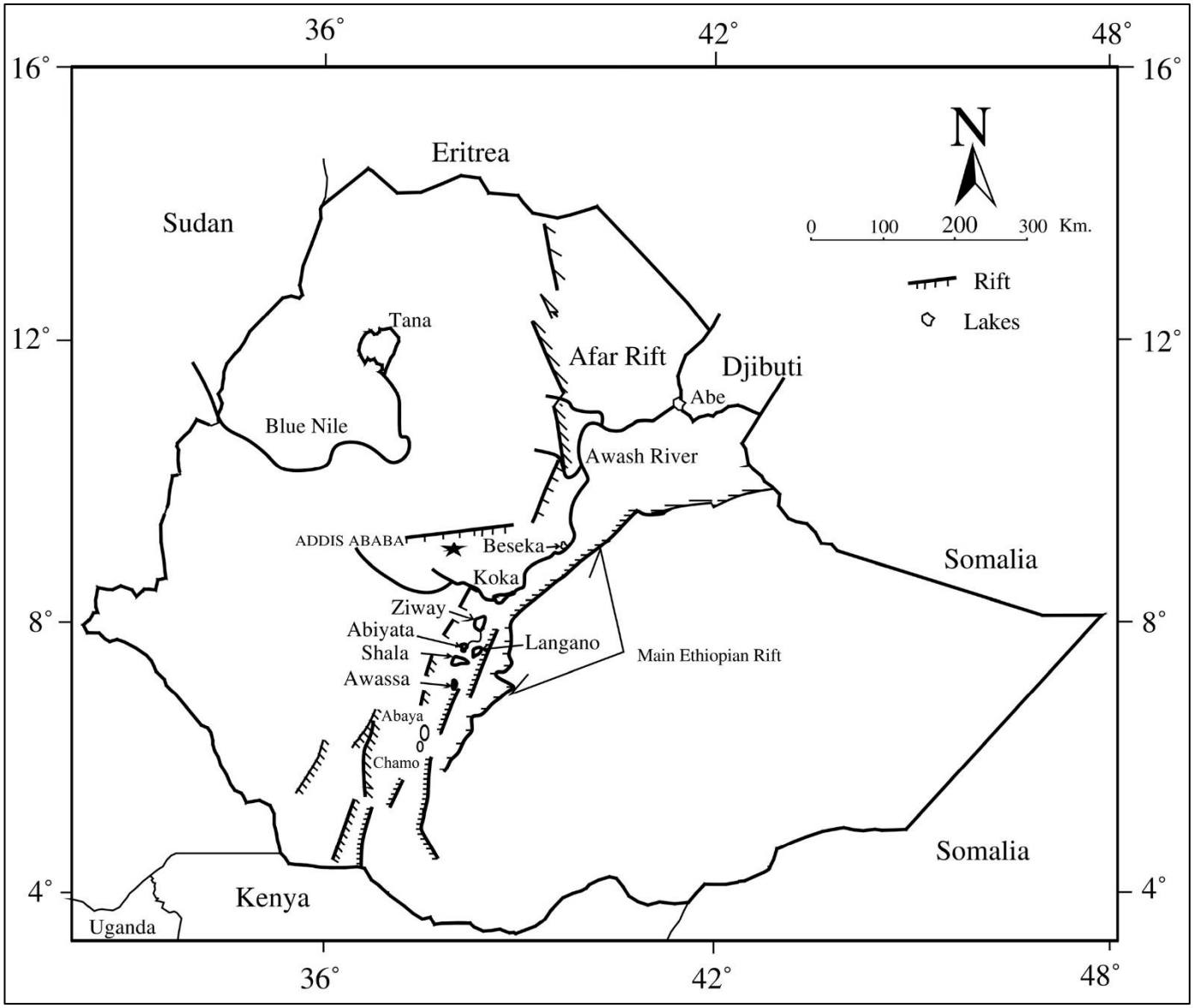

Figure2. 2: The major Earthquake-causative tectonic features Ethiopia (Mulugeta Dadi, 2015).

2.3 Hydrological setting

The aquifers of the northern and central part of Addis Ababa and in the mountainous area all around it are largely due to weathered and fractured volcanic rocks with minor sediments deposited between different series of lava flows. The aquifers at the southern part of the city are mainly young volcanic rocks of lava flow and tectonic fractures while the aquifers in the central part of the town shows confined groundwater conditions. Especially some places like Legedadi, Filwoha, Lideta and Kality areas exhibits artesian groundwater conditions. The confinement at the central part of the town varies from 23 to more than 100 meters. Most of the shallow groundwater potential areas north of the town are unconfined (Engida

Zemedagegnehu, 2001). The main structures, i.e. joints, fractures, and normal faults, are all related to the extensional rift tectonics in the area. A prime example is the Filwoha Fault, along which thermal activity is observed (Molla Demlie et al., 2007).

As (Engida Zemedagegnehu, 2001) reported, large proportion of the central part of Addis Ababa is under confined groundwater condition with groundwater depth varying from 0 to 40 meters. The depth is maximum along an elongated strip in the north-south direction (Filwoha, Lideta, Mekanisa, Lafto, Kailty) and the depth decreases both in the eastern and western direction from this elongated strip. There are also deeper groundwater areas of more than 120 meters depending on topography of the area. The groundwater flow within the town is variable with a general path in the north south direction. According to Tenalem Ayenew et al., (2008), the southern springs have direct connections with the high recharge in the northern wellhead protection areas.

CHAPTER THREE

THEORETICAL BACKGROUND OF METHODS OF INVESTIGATION

3.1 Introduction

Geophysical exploration utilizes different geophysical methods to detect any type of geological subsurface features like fractures, faults, cavities, weak zones, depth to bedrock and water saturation of the subsurface through indirect means by taking various physical measurements at surface, on air or within a borehole with cost effectively and efficient manner. Surface surveys are more commonly used for site investigations.

When utilizing multiple geophysical methods, each method provides information to better refine the conceptual model, minimize ambiguities and allow against one method failing to provide useful data than a single geophysical method. The selection of geophysical methods is depend on the objectives of the study, site geology, site access, experience of the researcher to the particular investigation and available cost.

In the current study, electrical resistivity tomography (specially polar or axial Dipole-Dipole electrical resistivity method), vertical electrical sounding (VES) and seismic refraction methods are employed. These methods can provide extensive and near continuous spatial data about the subsurface. However, each method has their own merit and demerit and may not be applicable in every situation. Site-specific geology, site access, and the presences of manmade features affect the geophysical measurement and determine the success of those particular geophysical methods to be used (Loke, 2004). Therefore, it is advisable to conduct integrated survey in case one technique fails or if there is a need to fill in data gaps in another one. The basic theory of each geophysical method employed in the present thesis are described briefly in the next sections.

3.2. The Electric Resistivity Method

3.2.1. Basic theory and principles

Electrical prospecting involves the detection of subsurface effects produced by electric current flow in the ground. The most common used methods for measuring Earth resistivity are those in which current is driven through the ground using galvanic contact. Generally, four terminal electrode arrays are used since the effect of material near the current contacts can be minimized. Current is driven through one pair of electrodes (A and B, Figure 3.1) and the potential established in the Earth by this current is measured with the second pair of electrodes (M and N) connected to a sensitive voltmeter. It is then possible to determine an effective or apparent resistivity of the subsurface (Shendi, 2008).

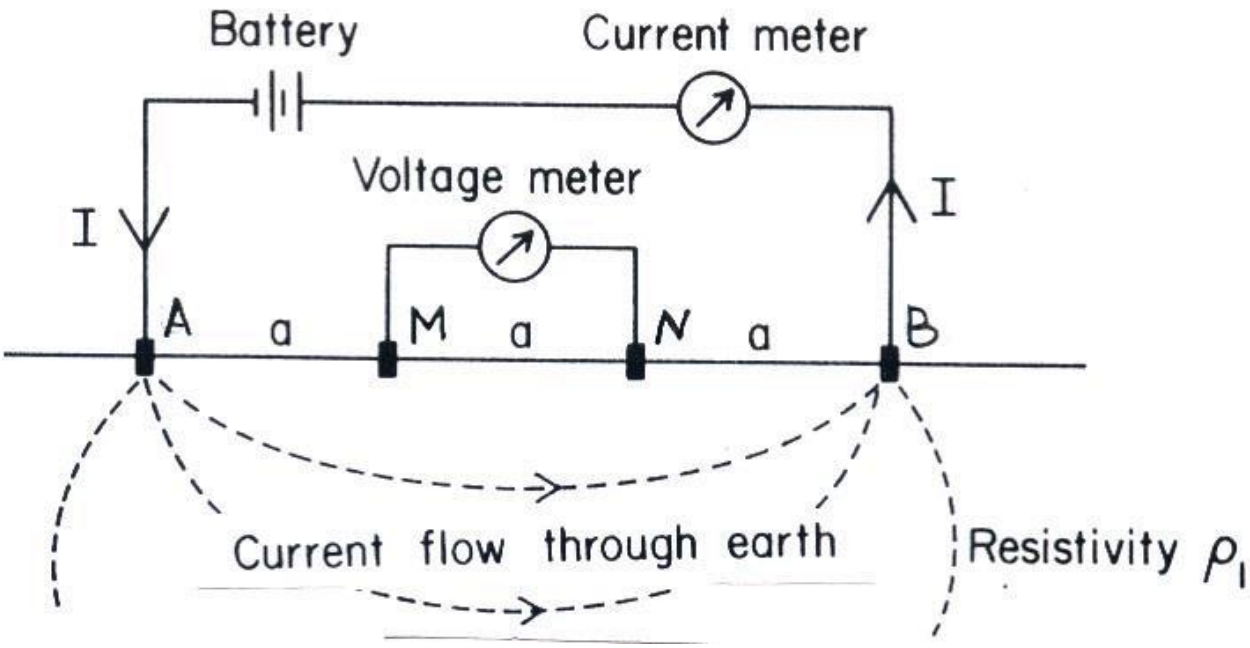

Figure3. 1: Arrangement of electrodes to flow electric current through the Earth

According to Loke (2004), the fundamental physical law used in resistivity surveys is Ohm's Law that governs the flow of current in the ground. The equation for Ohm's Law in vector form for current flow in a continuous medium is given by

$$\vec{J} = \sigma \vec{E} \qquad 3.1$$

where σ is the conductivity of the medium, J is the current density and E is the electric field intensity. In practice, what is measured is the electric field potential. We note that in geophysical surveys the medium resistivity ρ, which is equals to the reciprocal of the conductivity (ρ=1/σ), is more commonly used. The relationship between the electric potential and the field intensity is given by

$$E = -\nabla\Phi \qquad 3.2$$

Combining equations the above equations, one gets

$$\vec{J} = -\sigma \nabla\phi \qquad 3.3$$

For a homogeneous subsurface and a single point current source on the ground surface the current flows radially away from the source, and the potential varies inversely with distance from the current source. The equipotential surfaces have a hemisphere shape, and the current flow is perpendicular to the equipotential

surface. The current distribution is equal everywhere on this surface which is also called an equipotential surface. Starting with Ohm's law.

$$V = I\ R$$

And defining the resistance R in terms of the resistivity P and the area of the shell (equipotential surface), the potential difference across the shell is

$$di = i(R) = I\left(\frac{\rho l}{A}\right) = I\left(\frac{\rho dl}{2\pi r}\right)$$

where:

V = is the voltage (or electrical potential),

I = is the current,

ρ= is the resistivity and

r = is the radius of the equipotential surface.

Integrating the above equation and setting the potential at infinity to zero, the electric potential at a distance r from the source is given by

$$\phi = \frac{\rho I}{2\pi r} \qquad 3.4$$

where r is the distance of a point in the medium (including the ground surface) from the electrode.

In practice, all resistivity surveys use at least two current electrodes, a positive current source and a negative current sink to inject current into the ground. The potential values have a symmetrical pattern about the vertical plane at the mid-point between the two electrodes. The potential value in the medium from such a pair is given by

$$\phi = \frac{\rho I}{2\pi}\left[\frac{1}{r_{C_1}} - \frac{1}{r_{C_2}}\right] \qquad (3.5)$$

where rC1 and rC2 are distances of the point from the first and second current electrodes.

In practical surveys, the potential difference between two points (normally on the ground surface) is measured. A typical arrangement with 4- electrodes is shown in Figure 3.1. The potential difference is then given by

$$\Delta\phi = \frac{I\rho}{2\pi}\left[\frac{1}{r_{AM}} - \frac{1}{r_{BM}} - \frac{1}{r_{AN}} + \frac{1}{r_{BM}}\right] \tag{3.6}$$

From the current (I) and potential (∆∅) values, an apparent resistivity (ρa) value is calculated.

$$\rho_a = K\frac{\Delta\phi}{I} \tag{3.7}$$

$$\text{where} \quad k = \frac{2\pi}{\left[\frac{1}{r_{AM}} - \frac{1}{r_{BM}} - \frac{1}{r_{AN}} + \frac{1}{r_{BM}}\right]}$$

K is a geometric factor that depends on the arrangement of the four electrodes. Resistivity measuring instruments normally give a resistance value, R = ∆∅/I, so in practice the apparent resistivity value is calculated by

$$\rho_a = KR \tag{3.8}$$

If the measurement of (ρ) is made over a homogeneous and isotropic material, then the value of (ρ) computed from the above equation will be the true resistivity while if the medium is inhomogeneous and (or) anisotropic then the resistivity computed is called an apparent resistivity and is denoted by ρ_a.

3.2.2. The relationship between geology and Electrical resistivity

Electrical resistivity surveys give a picture of the subsurface resistivity distribution. To convert the resistivity picture into a geological picture, some knowledge of typical resistivity values for different types of subsurface materials and the geology of the area surveyed, is important (Loke, 2000).

The electrical resistivity of subsurface materials is a function of a number of soil or rock properties including the nature of the solid constituents (particle size distribution, mineralogy), arrangement of voids (porosity, pore size distribution, connectivity), degree of water saturation or water content, electrical resistivity of the

fluid (solute concentration) and temperature. Air medium is an insulator (i.e. infinitively resistive), water solution resistivity is a function of its ionic concentration, and the resistivity of solid grains is related to the electrical charge density at the surface of the constituents. These parameters affect the electrical resistivity, but in different ways and to different extents. Electrical resistivity experiments have been performed to establish relationships between the electrical resistivity and each of these soil or rock characteristics (Cousinet al., 2005).The resistivity values of common rocks, soil and minerals are shown in Figure 3.2.

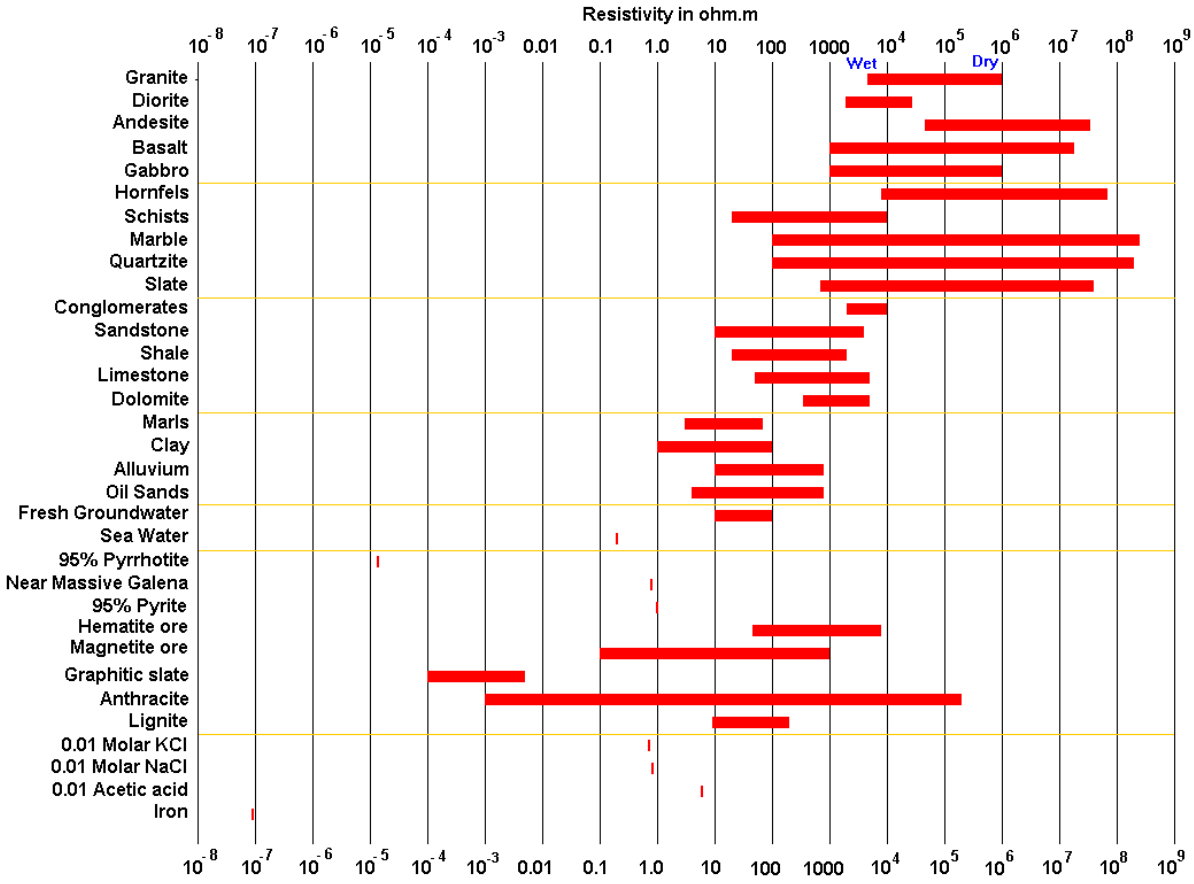

Figure3. 2: The resistivity of rocks, soils and minerals (Loke, 2004)

3.2.3. Useable techniques of electrical resistivity

3.2.3.1. Vertical Electrical Sounding (VES)

Vertical Electrical Sounding (VES) is one of the classical direct current (DC) geo-electrical prospecting techniques, together with the electrical resistivity profiling method. VES is used to determine the subsurface resistivity variation with depth and is applied in areas where the terrain is assumed to be horizontally layered, with very little or no lateral resistivity variations. The resulting apparent resistivity (ρ_a) sounding curves are usually interpreted using 1-D Earth models, characterized by a stepwise variation of the true resistivity with

depth (succession of N homogeneous and isotropic layers with true resistivityρ_1,ρ_2, …, ρ_N and thicknesses h_1, h_2, …, h_{N-1} or, alternately, depths to the layers interfaces z_1, z_2, …, z_{N-1}; the last layer of the model is considered infinitely extending downwards) (Niculescu, 2018). In this works, the geophysical resistivity technique using the vertical electrical sounding (VES) variation using the Schlumberger electrode array was employed.

The Schlumberger Array

The Schlumberger array (Figure 3.3), consists of four collinear electrodes. The outer two electrodes are current (source) electrodes while the inner two electrodes are the potential (receiver) electrodes. The potential electrodes are installed at the center of the electrode array with a small separation, typically less than one fifth of the spacing between the current electrodes. The current electrodes are increased to a greater separation during the survey while the potential electrodes remain in the same position until the observed voltage becomes too small to measure.

The advantages of the Schlumberger array are that fewer electrodes need to be moved for each sounding and the cable length for the potential electrodes is shorter. Schlumberger soundings generally have better resolution, greater probing depth, and less time-consuming field deployment than the others. The disadvantages are that long current electrode cables are required, the recording instrument needs to be very sensitive, and the array may be difficult or confusing to coordinate amongst the field crew (Hassan et al., 2017).

$$\rho_a = \frac{V}{I}\pi\frac{b(b+a)}{a} \approx \frac{V}{I}\pi\frac{b^2}{a}, \quad if\ a << b$$

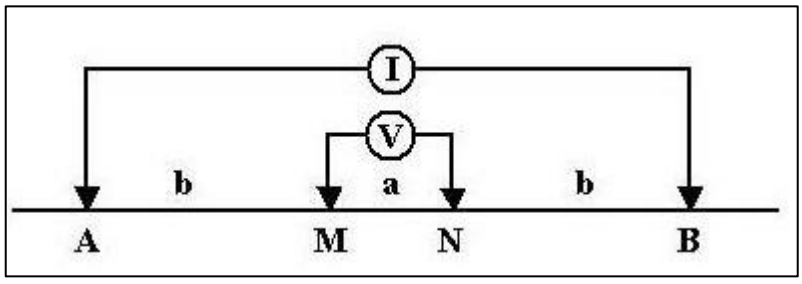

Figure3. 3: The Schlumberger electrode arrangement.

3.2.3.2. Interpretation of Vertical Electrical Sounding

Quantitative interpretation of geo-electrical data aims to delineate the true resistivity values and thicknesses of the sequential strata of subsurface section; the measured field data being represented by plotting the half

current electrode spacing (AB/2) against apparent resistivity values. There are two techniques of quantitative interpretation. The first one is the manual interpretation, which includes two methods and depends on using two layer standard curves and generalized Cagniard graphs; while the second one is the analytical interpretation- a technique which depends on using the results of manual interpretation as an initial model to compute the true resistivity values and thicknesses by using computer program final results (Araffa et al., 2019).

The interpretation problem for VES data is to use the curve of apparent resistivity versus electrode spacing, plotted from field measurements, to obtain the parameters of the geo-electrical section: the layers resistivity and thicknesses. From a given set of layer parameters, it is always possible to compute the apparent resistivity as a function of electrode spacing (the VES curve). To deal with the problem of ambiguity, the interpreter should check all interpretations by computing the theoretical VES curve for the interpreted section and comparing it with the field curve. The test of geological reasonableness should be applied. In particular, interpreted thin beds with unreasonably high resistivity contrasts are likely to be artifacts of interpretation rather than real features. Adjustments to the interpreted values may be made on the basis of the computed VES curves and checked by computing the new curves. Because of the accuracy limitations caused by instrumental and geological factors, effort should not be wasted on excessive refinement of the interpretation. (Araffa et al., 2019).

Standard two-layer curves for the Schlumberger array are plotted on a logarithmic scale, both horizontally and vertically, and are normalized by plotting the ratio of apparent resistivity to the first layer resistivity ($\frac{\rho_a}{\rho_1}$) against the ratio of electrode spacing to the first layer thickness ($\frac{d_a}{d_1}$) (Figure 3.4). Each curve of the family represents one value of the parameter *k*, which is defined by

$$k = \frac{\rho_2 - \rho_1}{\rho_2 + \rho_1} \qquad 3.9$$

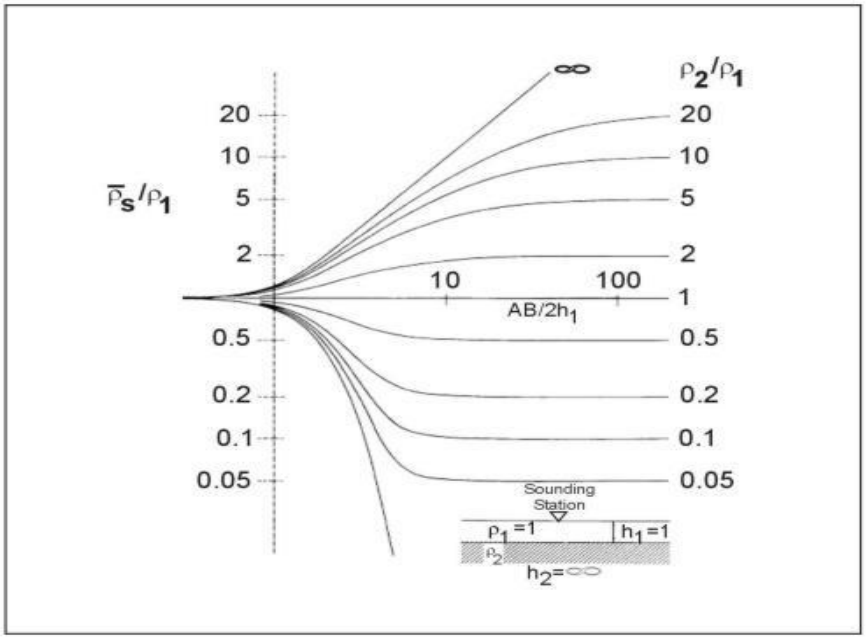

Figure3. 4: Two-layer master curves for Schlumberger array (Shendi, 2008)

Where three or more strata of contrasting resistivity are present, the VES curves are more complex than the two-layer curves. For three layers, there are four possible types of VES curves, as shown in Figure 3.5, depending on the nature of the successive resistivity contrasts. The classification of these curves is found in literature with the notations H, K, A, and Q. These symbols correspond respectively to bowl-type curves, which occur with an intermediate layer of lower resistivity than layers 1 or 3; bell-type curves, where the intermediate layer is of higher resistivity; ascending curves, where resistivity successively increase; and descending curves, where resistivity successively decrease (Shendi, 2008). With four layers, another curve segment is present, so that 16 curve types can be identified: HK for a bowl-bell curve, AA for a monotonically ascending curve, and so on.

- A-Type or Minimum type ($\rho1>\rho2<\rho3$)
- K-type or Maximum type ($\rho1<\rho2>\rho3$)
- A-type or Double ascending ($\rho1<\rho2<\rho3$)
- Q-type or Double descending ($\rho1>\rho2>\rho3$)

Much larger sets of curves are required to represent the increased number of possible combinations of resistivity and layer thicknesses. Direct curve fitting is time consuming. Therefore, it is better use auxiliary point techniques. The Auxiliary Point Method, which requires the use of a small set of auxiliary curves and

some constructions, can use two or three-layer curves for complete interpretation of VES curves of more layers (Shendi, 2008).

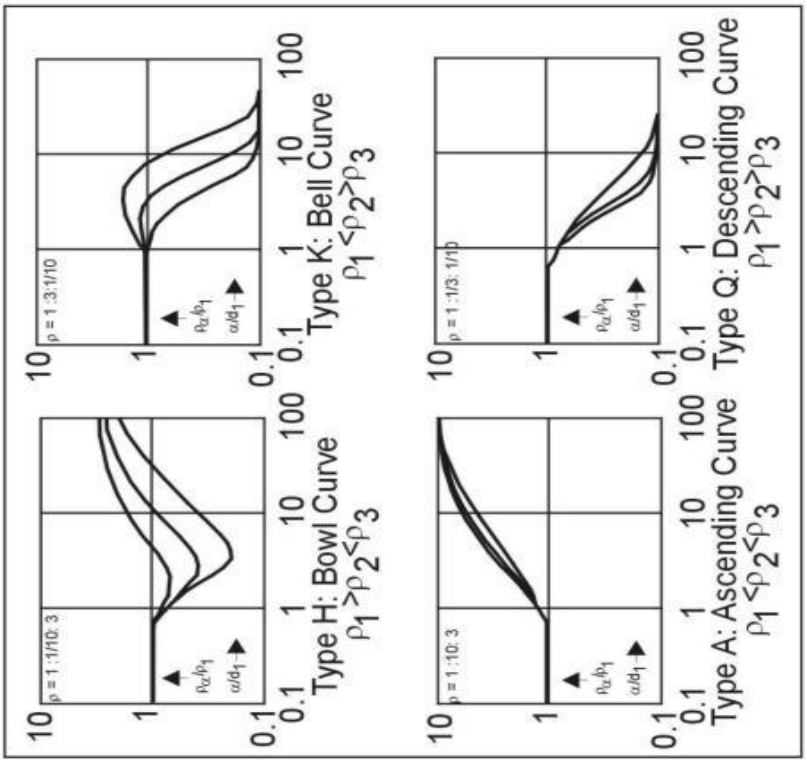

Figure3. 5: The four types of three-layer VES curves; the three sample curves for each of the four types represent values of d2/d1= 1/3, 1 and 3 respectively (Shendi, 2008).

3.2.3.3. 2D Electrical Resistivity Tomography

Electrical imaging is a surveying technique for an area of complex geology where the use of resistivity sounding and other techniques are unsuitable for providing detailed subsurface information in a limited area (Barker, 1999). Electrical resistivity surveys are normally carried out with multi-electrode system. Such surveys use a number of electrodes (25 to 100) deployed in a straight line with constant spacing, connected to the measuring unit with a multicore cable. The Electrical Resistivity Tomography (ERT), as such measurement is called, is an active geophysical method that can provide 2D or 3D images of the distribution of the electrical resistivity in the subsoil. The analysis and interpretation of these electrical images allow the identification of resistivity contrasts that can be mainly due to the lithological nature of the terrains and the water content variation. The in-field procedure includes the use of a multi-electrode cable, laid out on the ground, to which a number of steel electrodes are connected at a fixed distance according to a specific electrode configuration. The electrodes are used both for the injection of the current (I) in the subsoil and the measurement of the voltage (V). Knowing the I and V values and the geometrical coefficient depending on

the electrode configuration used, the apparent resistivity values characterizing the subsoil investigated can be calculated (Perrone et al., 2014). The possible arrangement of common electrodes array and geometric factor are shown in the Figure 3.7.

Electrical Resistivity Tomography (ERT) which is a non-invasive method, is extremely useful for understanding the sub-surface formations and for depth estimations of natural resources. High-resolution Electrical Resistivity Tomography (HERT) surveys play an important role in data acquisition especially in noisy areas. This is achieved by over lapping data levels with different combinations of Dipole lengths and Dipole's separations, as a whole, when Dipole–Dipole array is applied. The most applicable one is dipole-dipole array electrode configuration, where all the four electrodes and in line, shown in Figure 3.7. The number of data points produced by such high resolution survey is more than twice that obtained with a conventional array in routine application and hence a better area coverage and resolution can be achieved for most applications (Kumar et al., 2015).

In dipole-dipole survey, the data of measured resistivity are plotted at corresponding points to the value of n (n = 1,2,3,4,5,6, etc.) with the apparent depth level, so that pseudo depth section contours of resistivity variations to lateral direction toward the direction of the apparent depth can be made. Both current and potential electrodes are separated by distance "a"- the dipole length, while the centers of the current and the electrode potential are separated section as far as "n_a", where n is an integer. Variations of "n" is used to get a certain depth, greater "n" will obtain bigger depth. The level of range sensitivity of the dipole-dipole array is affected by the value of "a" and "n" variation as shown in equation (3.10).

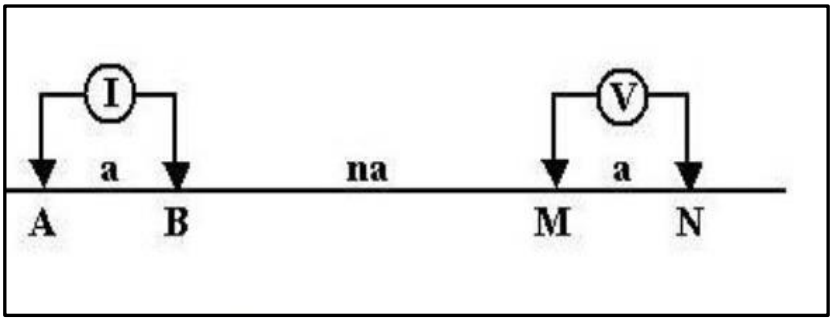

Figure3. 6: The Dipole-Dipole electrode setup.

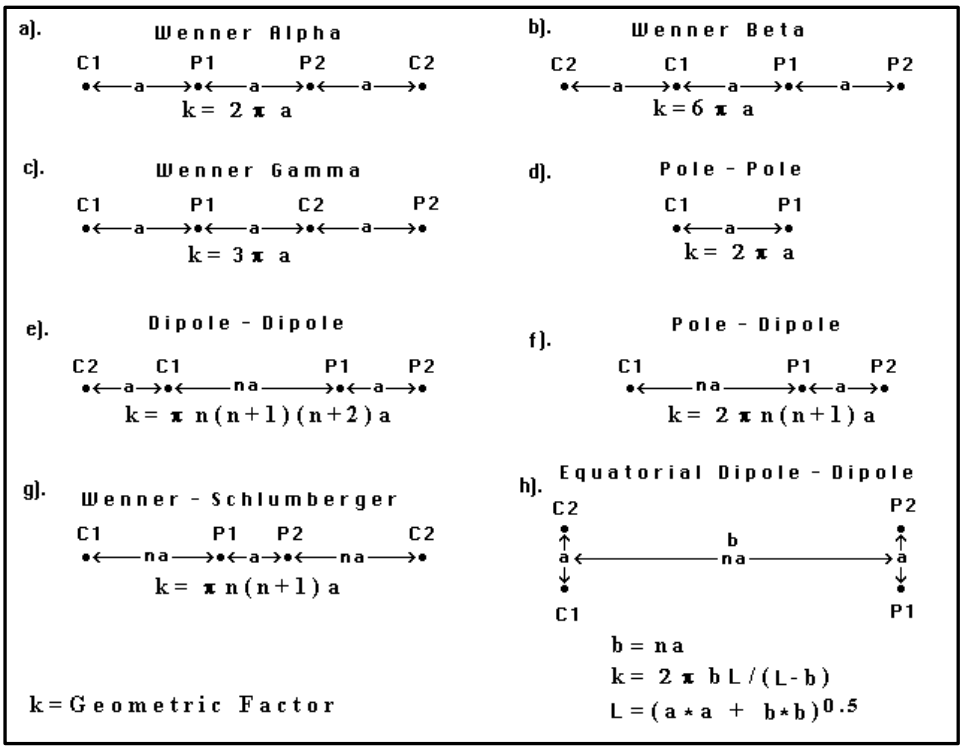

Figure3. 7: Common arrays used in resistivity surveys and their geometric factors (Loke, 2000).

The apparent resistivity is obtained from the expression (equation (3.8)) as

$$\rho_a = k\frac{V}{I}$$

where 'k' is the geometric factor for the array describing the way the four electrodes are disposed over the Earth's surface and for axial dipole-dipole array takes the form

$$k = \pi an(n+1)(n+2)$$

and hence , the measured apparent resistivity

$$\rho_a = \frac{V}{I}an(n=1)(n+2) \qquad 3.10$$

The results of measurement using more spaces between current and potential electrode (the product 'na') will give deeper information on subsurface structure (Octova et al., 2016). Thus, the dipole-dipole configuration can be effective in mapping subsurface layers whose physical properties vary, both laterally and vertically. The measurement procedure and measured data points are as shown in Figure 3.6.

The value geometric factor dipole-dipole is $k = \pi an(n+1)(n+2)$

$$\rho_a = \frac{V}{I}\, k$$

$$\rho_a = \frac{V}{I}\, an(n+1)(n+2) \ldots\ldots\ldots\ldots\ldots\ldots\ldots 3.10$$

The results of measurement using more spaces between current and potential electrode will give deeper information on subsurface structure (Octova et al., 2016). Thus, the dipole-dipole configuration can be effectively in mapping, both laterally and vertically as shown in Figure 3.8.

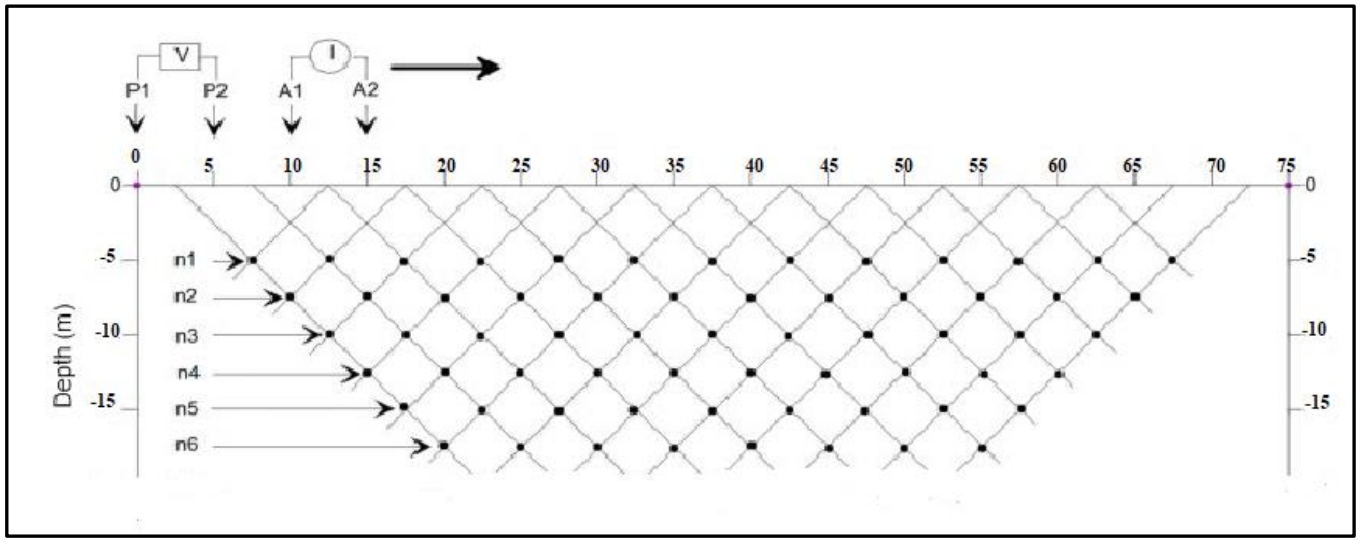

Figure3. 8: Electrode array of dipole-dipole profiling survey with depth information included.

According to Kumar et al., (2015), in each location one obtains three images, namely, the top one indicates the observed image and the middle one indicates the computed one whereas the bottom one indicates the true resistivity image which is obtained after applying the inversion shown in Figure 4.4. As it is not possible to measure physically the true resistivity in the field, the other alternative procedure to get a true resistivity image of the sub-surface is to apply the method of Inversion to the observed apparent resistivity data so that the true resistivity image is obtained. The inversion procedure is applied by using either the least square method or the Finite Element or Finite Difference methods.

The 2D electrical resistivity tomography data can be processed with the Res2dinv software to produce a two dimensional model of the subsurface from the apparent electrical resistivity data. The inversion routine uses a non-linear least-squares optimization technique. The optimization technique tries to minimize the difference between the calculated and measured apparent resistivity values by adjusting the resistivity of the model Earth subsurface blocks. A measure of this difference is often given after 3-5 iterations by the root-mean-square (RMS) error (Ugwu et al., 2013).

Thus the dipole-dipole array is very sensitive to horizontal changes in resistivity, but relatively insensitive to vertical changes in the resistivity. That means that it is good in mapping vertical structures, such as dykes and cavities, but relatively poor in mapping horizontal structures such as sills or sedimentary layers. The median depth of investigation of this array also depends on the "n" factor, as well as the "a" factor (Table 3.1). In general, this array has a shallower depth of investigation compared to the Wenner array (Loke, 2000).

One possible disadvantage of this array is the very small signal strength for large values of the "n" factor. The voltage is inversely proportional to the cube of the "n" factor. This means that for the same current, the voltage measured by the resistivity meter drops by about 200 times when "n" is increased from 1 to 6. One method to overcome this problem is to increase the "a" spacing between the C1-C2 (and P1-P2) dipole pair to reduce the drop in the potential when the overall length of the array is increased to increase the depth of investigation. To use this array effectively, the resistivity meter should have comparatively high sensitivity and very good noise rejection circuitry, and there should be good contact between the electrodes and the ground in the survey. With the proper field equipment and survey techniques, this array has been successfully used in many areas to detect structures such as cavities where the good horizontal resolution of this array is a major advantage (Loke, 2000).

Table3. 1: The median depth of investigation (z e) for the different arrays. L is the total length of the array. Note identical values of Z_e/a for the Wenner-Schlumberger and pole-dipole arrays (Loke, 2000)

Array type	**z_e/a**	**z_e/L**
Wenner Alpha	0.519	0.173
Wenner Beta	0.416	0.139
Wenner Gamma	0.594	0.198
Dipole-dipole n = 1	0.416	0.139
n = 2	0.697	0.174
n = 3	0.962	0.192
n = 4	1.220	0.203
n = 5	1.476	0.211
n = 6	1.730	0.216
Equatorial dipole-dipole		
n = 1	0.451	0.319
n = 2	0.809	0.362
n = 3	1.180	0.373
n = 4	1.556	0.377
Wenner - Schlumberger		
n = 1	0.52	0.173
n = 2	0.93	0.186

n = 3	1.32	0.189
n = 4	1.71	0.190
n = 5	2.09	0.190
n = 6	2.48	0.190
Pole-dipole n = 1	0.52	
n = 2	0.93	
n = 3	1.32	
n = 4	1.71	
n = 5	2.09	
n = 6	2.48	
Pole-Pole	0.867	

3.3 Fundamental Principle of Seismic Method

Seismic methods are the most commonly conducted geophysical surveys for engineering investigations. Seismic waves are parcels of elastic strain energy that propagate outwards from a seismic source such as an earthquake or an explosion. Sources suitable for seismic surveying usually generate short-lived wave trains, known as pulses. The propagation velocities of seismic pulses are determined by the elastic moduli and densities of the materials through which they pass (Kearey et al., 2002).

In isotropic and homogeneous solids, the mode of propagation of a P-wave is always longitudinal; thus, the particles in the solid have vibrations along or parallel to the travel direction of the wave energy. The velocity of P-waves in a homogeneous isotropic medium is given by equation (3.11):

$$V_p = \sqrt{\frac{K + \frac{4}{3}\mu}{\rho}} = \sqrt{\frac{\lambda + 2\mu}{\rho}} \qquad 3.11$$

and the velocity Vs of a shear body wave, which involves a pure shear strain, is given by

$$V_s = \sqrt{\frac{\mu}{\rho}} \qquad 3.12$$

where K is the bulk modulus (the modulus of incompressibility), μ is the shear modulus (modulus of rigidity, sometimes denoted as G and also called the second Lame parameter), ρ is the density of the material through which the wave propagates, and λ is the first Lame parameter(Sharafeldin et al., 2017).

There are two techniques of seismic method which are seismic refraction and seismic reflection techniques. In this study, the technique employed is used seismic refraction, therefore, detailed explanation of the basic principle of seismic refraction technique is presented as follows (Kearey et al., 2002).

Seismic Refraction Technique

The seismic refraction technique is one geophysical method which is frequently used to determine the characteristics of soils and rocks. The technique finds application in the determination of rock competence for engineering application, depth to bedrock, groundwater exploration, crustal structure and tectonics (Redpath, 1973).

The refraction method consists of measuring (at known points along the surface of the ground) the travel times of compressional waves generated by an impulsive energy source. The energy source is usually a small explosive charge and the energy is detected, amplified, and recorded on surface at a series of receivers called geophones spaced at regular intervals. The instant of the explosion, or "zero-time," is recorded on the record of arriving pulses. The raw data, therefore, consist of travel times and distances, and this time-distance information is then manipulated to convert it into the format of velocity variations with depth. The energy generated either travels directly through the upper layer (direct arrivals), or travel down through the various layers before returning to the surface (refracted arrivals) (Redpath, 1973) as shown in Figure3.9.

.

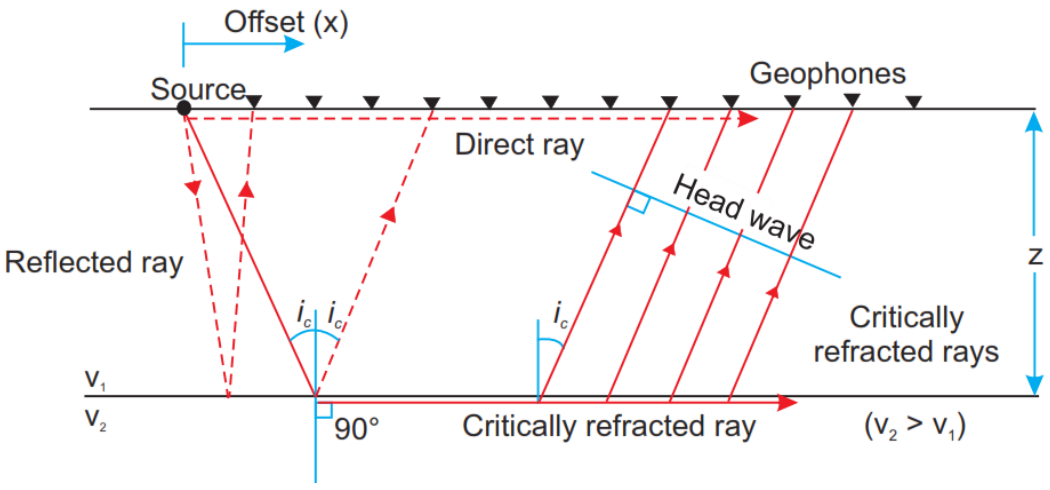

Figure3. 9: propagation of Seismic refraction energy through subsurface

According to Redpath (1973), the propagation of seismic energy through subsurface layers is described essentially by the same rules that govern the propagation of light rays through transparent media. The refraction or angular deviation that a light ray or seismic pulse undergoes when passing from one material to another depends upon the ratio of the transmission velocities of the two materials. The fundamental law that describes the refraction of light ray is Snell's law and this together with the phenomenon of critical incidence is the physical foundation of seismic refraction surveys p-waves. Snell's law and critical incidence (i_c) are shown in Figure 3.10, and it shows a medium with a velocity V_1, underlain by a medium with a higher velocity V_2.

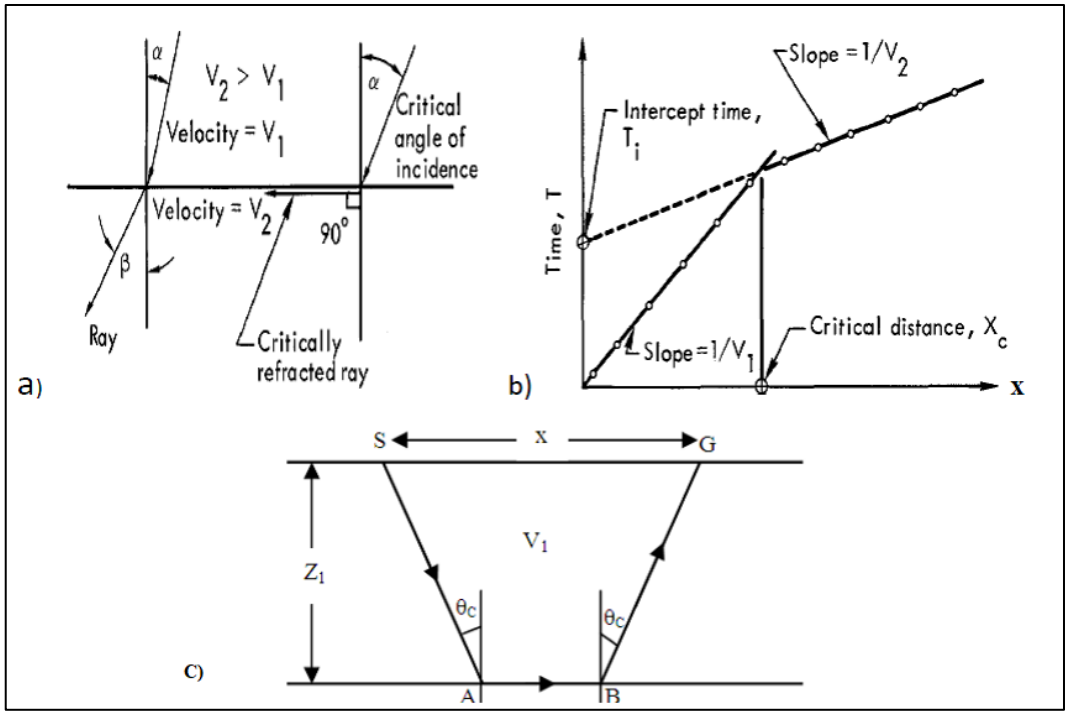

Figure3. 10: seismic refraction principles a) Snell's Law and refraction of ray transmitted across boundary between two media with different velocities, b) Travel-Time graph for two layer surface, c) A two layer horizontal stratified substratum (Redpath, 1973).

The theory of refraction seismic method is based on the combinations of Snell`s laws, Fermat's principle and Huygens's principle. Consequences of Snell`s law for the refracted wave in two layer medias with velocity V_1 and V_2 is expressed as:

i) when the velocity of the first layer and the second layer are the same ($V_1 = V_2$), the waves go straight and there is no refraction (constant velocity).

ii) when $V_2 > V_1$, the wave is refracted away from the normal and there is a possibility to measure the refracted wave at the surface. In this case seismic refraction will work.

iii) when $V_2 < V_1$, the wave is refracted towards the normal and there is a no possibility to measure the refracted wave at the surface.

Hence, the seismic refraction method faces problems in the case of inverted layer and blind zone (i.e. in case of velocity inversion, when there is a low velocity layer beneath a higher velocity layer and thin layer).

Snell's law $$\frac{\sin\alpha}{\sin\beta} = \frac{V_1}{V_2} \qquad 3.13$$

Critical incidence occurs when β =90°, therefore,

$$\sin\alpha = \frac{V_1}{V_2}$$

Using Figure3.10 c, one considers the wave SA which 'hits' the layer boundary at the critical angle θc. The total travel time for the refraction signal to travel from the source 'S' to the geophone 'G' is expressed as

$$T_{SG} = T_{SA} + T_{AB} + T_{BG} \qquad 3.14$$

Which also can be expressed in terms of displacement and velocity

$$T_{SG} = \frac{SA}{V_1} + \frac{AB}{V_2} + \frac{BG}{V_1}$$

$$SA = BG = \frac{Z}{\cos\theta_C} \quad \text{and} \quad AB = x - 2Z_1 \tan\theta_C$$

Therefore, total travel time

$$T_{SG} = \frac{2Z_1}{V_1\cos\theta_C} + \frac{2Z_1\tan\theta_C}{V_2}$$

$$\sin^2\theta + \cos^2\theta = 1$$

$$T_{SG} = \frac{x}{V_2} + \frac{2Z_1\cos\theta_C}{V_1} \qquad 3.15$$

Letting X = 0, then T becomes the intercept time (T_i), and we can rewrite the last expression as:

$$Z_1 = \frac{T_i V_1}{2\cos\theta_C}$$

$$Z_1 = \frac{T_i V_1}{2\cos\left(\sin^{-1}\frac{V_1}{V_2}\right)} = \frac{T_i V_1 V_2}{2\sqrt{V_2^2 - V_1^2}} \qquad 3.16$$

where Z_1 is the thickness of the first layer.

The critical distance (X_c) is the point on the surface at which the direct wave and the head wave arrived simultaneously. Before the critical distance, the direct waves arrive first while beyond the critical distance, the head wave arrives first.

According to Fkirin et al., (2016), the multi-layered subsurface is considered as a many plane horizontal layer as shown in Figure 3.11.

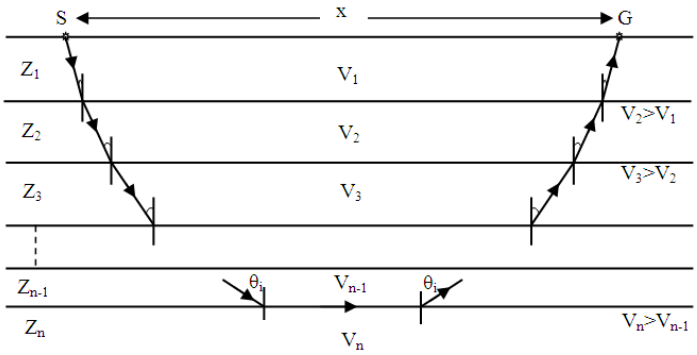

Figure3. 11: multi-layered horizontal stratified substratum

$$T_{SG} = \frac{X}{V_n} + \sum_{i=1}^{n-1} \frac{2Z_i \cos\theta_i}{V_i}$$

where 'n' is the number of layers, θ_i is the angle of incidence at the i^{th} interface and Z_i is the depth at the base of a layer of velocity V_i.

The generalized depth equation of the subsurface layers is also obtained as follows:

$$Z_i = \frac{T_i V_1 V_{i+1}}{2\sqrt{V_{i+1}^2 - V_1^2}} \qquad 3.17$$

3.3.1 The relationship between Geology and Seismic Velocity

By virtue of their various compositions, textures (e.g. grain shape and degree of sorting), porosities and contained pore fluids, rocks differ in their elastic moduli and densities and, hence, in their seismic velocities. Information on the compressional and shear wave velocities, V_p andV_s, of rock layers encountered by seismic surveys is important for two main reasons: firstly, it is necessary for the conversion of seismic wave travel times into depths; and secondly, it provides an indication of the lithology of a rock or, in some cases, the nature of the pore fluids contained within it (Kearey et al., 2002). Typical compressional wave velocity values and ranges for a wide variety of Earth materials are given in Table 3.2(Kearey et al., 2002).

Table3. 2: Compressional wave velocities in Earth materials (Kearey et al., 2002).

Earth materials	$\boldsymbol{V_p(Kms^{-1})}$
Unconsolidated materials	
Sand (dry)	0.2-1.0
Sand(water-saturated)	1.5-2.0
Clay	1.0-2.5
Glacial till(water saturated)	1.5-2.5
Permafrost	3.5-4.0
Sedimentary rock	
Sandstones	2.0-6.0
Tertiary sandstone	2.0-2.5
Pennant sandstone (Carboniferous)	4.0-4.5
Cambrian quartzite	5.5-6.0
Limestones	2.0-6.0
Cretaceous chalk	2.0-2.5
Jurassic oolites and bio-clastic limestones	3.0-4.0
Carboniferous limestone	5.0-5.5
Dolomites	2.5-6.5
Salt	4.5-5.0
Anhydrite	4.5-6.5

Gypsum	2.0-3.5
Igneous/Metamorphic rocks	
Granite	5.5-6.0
Gabbro	6.5-7.0
Ultramafic rocks	7.5-8.5
Serpentinite	5.5-6.5
Pore fluids	
Air	0.3
Water	1.4-1.5
Ice	3.4
Petroleum	1.3-1.4
Other materials	
Steel	6.1
Iron	5.8
Aluminum	6.6
Concreate	3.6

CHAPTER FOUR

FIELD DATA ACQUISITION, PROCESSING AND PRESENTATION

4.1. Survey layout and profile selection

To successfully carry out the primary electrical resistivity and seismic refraction data acquisition, systematic survey lines were selected within the study area. The selection of the profile lines is basically made with the consideration of site accessibility, local geological situation and investigation interest which is the objectives of the particular study. As shown in Figure 4.1, four sounding data points, distributed along one profile line, 2D imaging data along four profile lines and seismic refraction data along two lines have been collected. The selection of these survey lines were mainly determined by site accessibility as the area of the study has already been tampered with buildings, fences, foundation excavations and piling of construction material. The primary collected data set acquired from the field were processed using various geophysical modeling software packages and presented in the form of sections and maps. The next sections of this chapter outline the detailed description of each geophysical data acquisition, processing and presentation.

4.2 Electrical resistivity

4.2.1 Data acquisition and instrumentation

To determine the lateral and vertical electrical resistivity variation of the near surface geological features underling the studied building foundation site, vertical electrical sounding and 2D imaging survey were conducted. The field work of these both methods done in January to February. The data acquisition method and the instrument used for data collection for both survey are discussed in the following subsections.

4.2.1.1 Vertical Electrical Sounding (VES)

In order to determine the near surface vertical resistivity distribution of the subsurface over the building site, a Schlumberger configuration was used. The working procedure for this surveying is made by expanding both the current and potential electrodes symmetrically with respect to the sounding point. Four sounding points distributed along one profile line were carried out in the study site. The survey profile lies in the middle of two asphalt road and only about 15m far from the target site. The selection of this line is dictated by unavailability of linear space within the compounds of the building site. The distance between the sounding stations is 50m and the profile is oriented S to N direction. A Schlumberger configuration with a maximum half current electrode spacing of 220m (AB/2=220m) was utilized to investigate the ground to a depth of interest for geotechnical studies and examine the possibility of groundwater saturation of the subsurface at shallow depths.

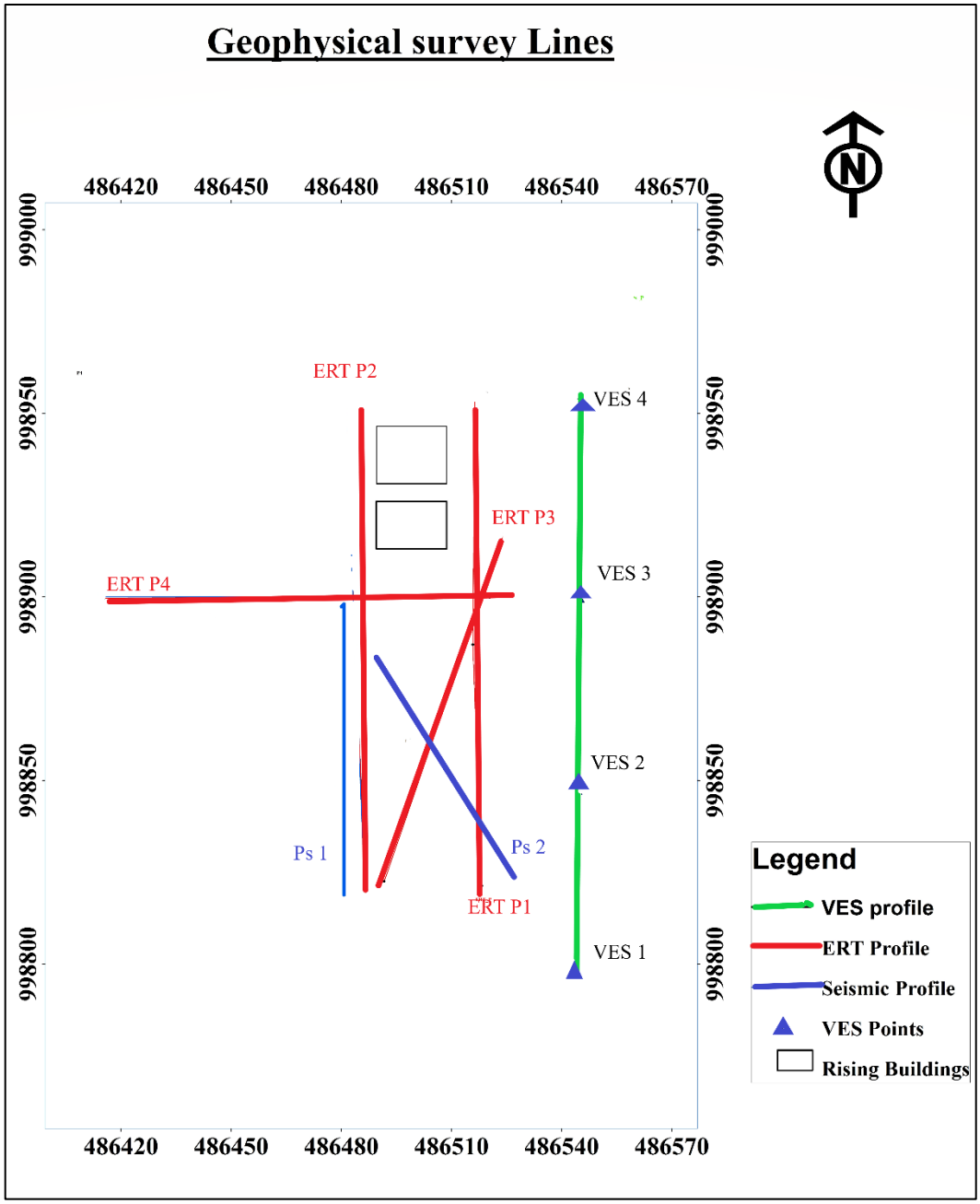

Figure 4. 1: The geophysical survey lines.

4.2.1.2 Electrical Resistivity Tomography (ERT)

This survey was conducted to know both the vertical and lateral heterogeneity of near surface features underlying the study area with a higher resolution. The array is known to give a better lateral resolution of the subsurface and it is expected that this feature of the array is to be exploited here. ERT data were collected along four profile lines with 130 m, 125m, 105m and 90m in length (Figure 4.1). The data acquisition was adopted by using axial dipole-dipole configuration with maximum unit electrode spacing of 5m interval and

six measurements/depth slices are taken (with n=1, 2, 3 . . ., 6) at each point. For all profiles, the total number of data point acquired are from 17 to 25 within the target site respectively. The orientation of profile line one and profile line two are nearly parallel and oriented S to N (almost parallel to the VES Line), the third profile line is perpendicular to profile lines one and two while the fourth profile line is slightly diagonal and is oriented SW to NE .Data acquisition of profile lines one and two are taken at the front and back side of the two rising buildings with a line spacing of 90m.

To collect both the ERT and VES data, the Italy made *PASI*-16GL EARTH RESISTIVITY METER, with P100-3 Energizer unit were utilized (Figure 4.2). The units are highly portable, rugged and simple for operation and utilize different accessories, such as stainless steel and copper wire cables and electrodes. The locations of the study area boundary, dipole- dipole profiles lines, electrical resistivity sounding points, geophone position, relative distance between surveyed points and shot points interims of Easting, Northing and elevations in unit of meter were recorded using the Garmin GPSMAP 64s receiver.

Figure4. 2: The electrical resistivity surveying instruments utilized in this study.

4.2.2 Data processing and presentation

4.2.2.1. Vertical electrical sounding

The primary VES data acquired from each sounding stations along the profile line with Schlumberger array were processed by using *IPI2WIN* software to obtain the initial model of the layer parameters which are thickness of layer and true resistivity. Then the result of initial model parameters obtained from *IPI2WIN* software were processed by using *WinResist* software (Figure 4.3). Finally the individual interpreted curves provide the parameters required for the preparation of the geo-electrical section. In addition to this, the raw apparent resistivity data in Z, length of survey in X and pseudo depth in Y axis are plotted by using the surfer

software package which results in what is known as a pseudo-depth section map of the entire area along the VES profile line.

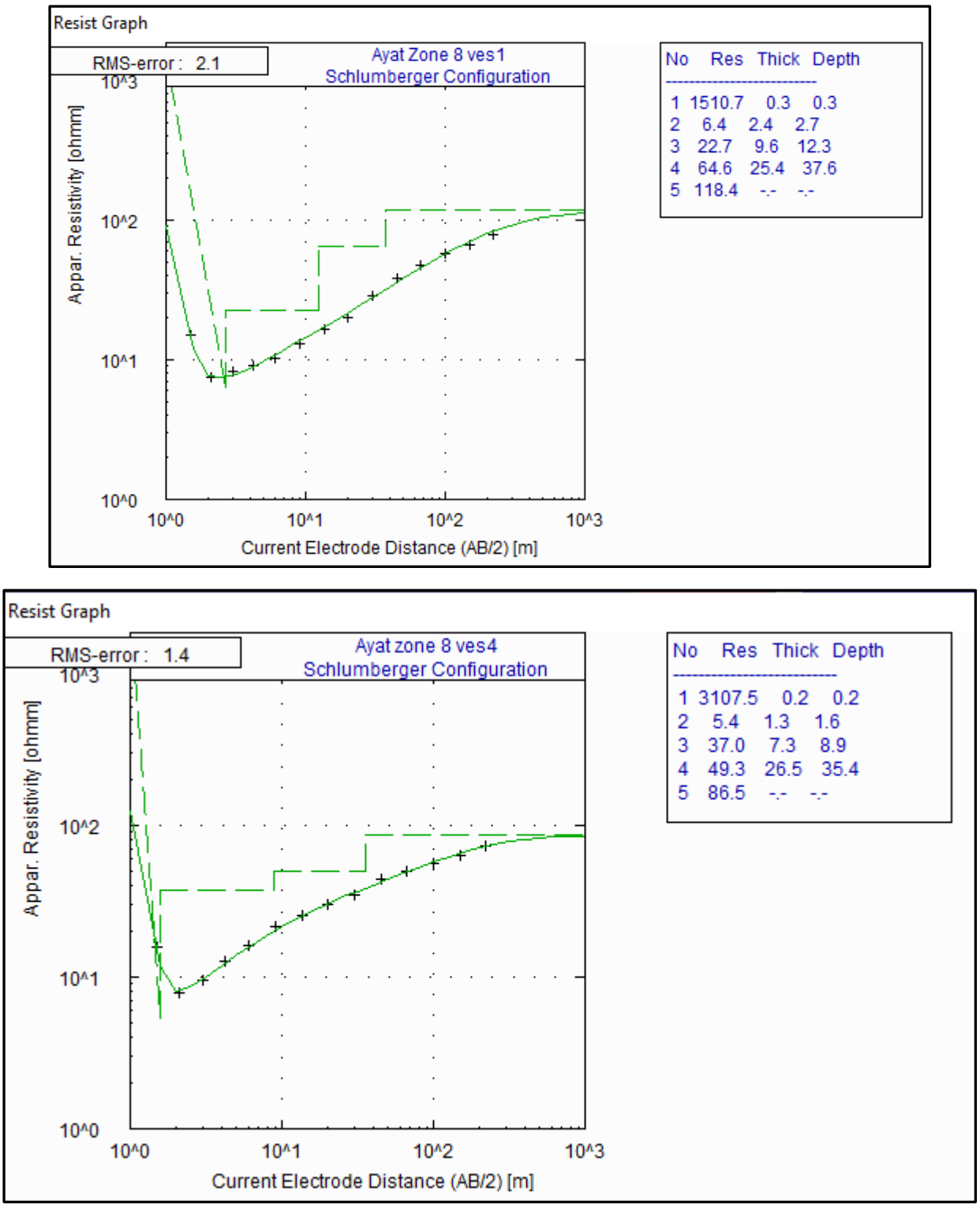

Figure4. 3 Examples of individual VES interpreted curves of VES1 and VES4.

From the illustration for results showing the VES data interpretation given in Figure 4.3, it is seen that data of good quality has been acquired from the field as witnessed by the low RMS error percentages indicated (2.1% for VES-1 and 1.4% for VES-4). The VES have been conveniently interpreted to give a 5-layer subsurface of varying resistivity and thickness.

4.2.2.1 Electrical Resistivity Tomography

Frist, the primary 2D electrical resistivity raw data acquired in the field were recorded in a note pad and processed by RES2DINVver.3.55 software. A total of 25, 24, 20 and 17 valid data points for Profile-1, Profile-2, Profile-3 and Profile-4, respectively, were processed separately for the inversion result. As a sample, for the data of Profile-4 which covers a 105m length, the measured apparent resistivity, calculated apparent resistivity pseudo section and inverse model resistivity section is shown in the Figure 4.4. When the 2D inversion software program has been applied to yield valid inversion result, 3 iterations have been executed to yield the section with an RMS error of 8.1%. Further iteration was not imposed on the data not to artificially introduce artifacts to the data and this percentage of error has been accepted.

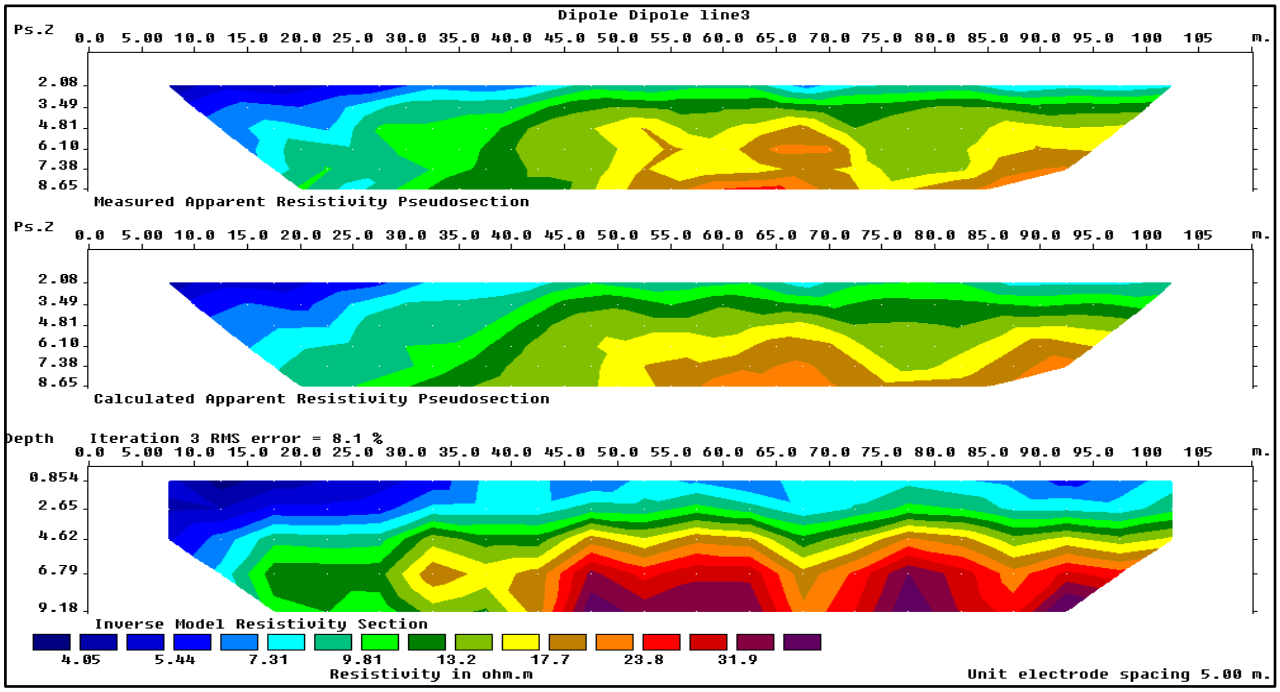

Figure4. 4 Measured, calculated and inverse 2D resistivity model of ERT Profile-4.

4.3. Seismic Refraction survey

4.3.1 Data acquisition and instrumentation

In this study, the seismic refraction survey conducted by using Geometrics 24 channel geode seismograph along two profiles lines and its field work is completed in June. The length of each profile is 48m and 2m geophone spacing was applied. In each profile line there were five shot points (5m far from the first geophone for the near forward shot, between geophone numbers 6 and 7, between geophone numbers 12 and 13 geophones, between number 18 and 19 geophones finally 5m far from the last geophone for the near reverse). In order to generate artificial seismic energy, a 10kg sledge hammer was utilized with metallic strike plate. For each shot point, the strike plate was pounded by the sledge hammer about five times and in some instances more strikes to enhance the seismic energy/ to facilitate signal stacking. The strike plate, sledge hammer, seismograph and geophones are connected by a means of seismic and trigger cables. The location of each successive geophones and shot points interims of easting, northing and elevation were taken with help of Garmin GPSMAP64s. The seismic refraction survey profiles are oriented N to S parallel to the first two ERT profiles with 5m spacing to the second ERT profile line. The second profile of seismic refraction is diagonal to ERT profiles and is in the direction of SE to NW. The instruments utilized to do seismic refraction survey are as illustrated in Figure 4.5.

Figure4. 5: Seismic refraction survey instruments.

4.3.2 Processing and presentation of seismic data

First, the primary seismic refraction data acquired in the field was taken from the computer which is used to display the wave characteristics during the field work. Next, the first arrival times (first breaks) of the wave form data recorded in the field was picked with the help of the *PICKWIN ver.4.0.0.4 2008 software* (Fkirin et al., (2016). Then, the picked arrival times were saved to generate the travel time curves (distance-time plots) and further processed with the help of *Plotrefa_ee ver.2.9.1.2* software (Fkirin et al., (2016) to invert the travel time curve into the velocity and layer model of the subsurface. Figures 4.6 give examples of the outputs of the software. The seismic refraction data acquisition and processing steps and processes are as summarized in Table 4.1.

Table4. 1: Seismic refraction data acquisition and processing summary.

Instrument	geometrics 24 channel geode seismograph
Source	Sledge hammer (10kg)
Geophone	Vertical
Geophone Spacing	2m
Initial shot point	5m far from first geophone
Shot point interval	11m
Data format	SEG2
Software to process	PICKWIN ver.4.0.0.4 2008 and Plotrefa_ee ver.2.9.1.2

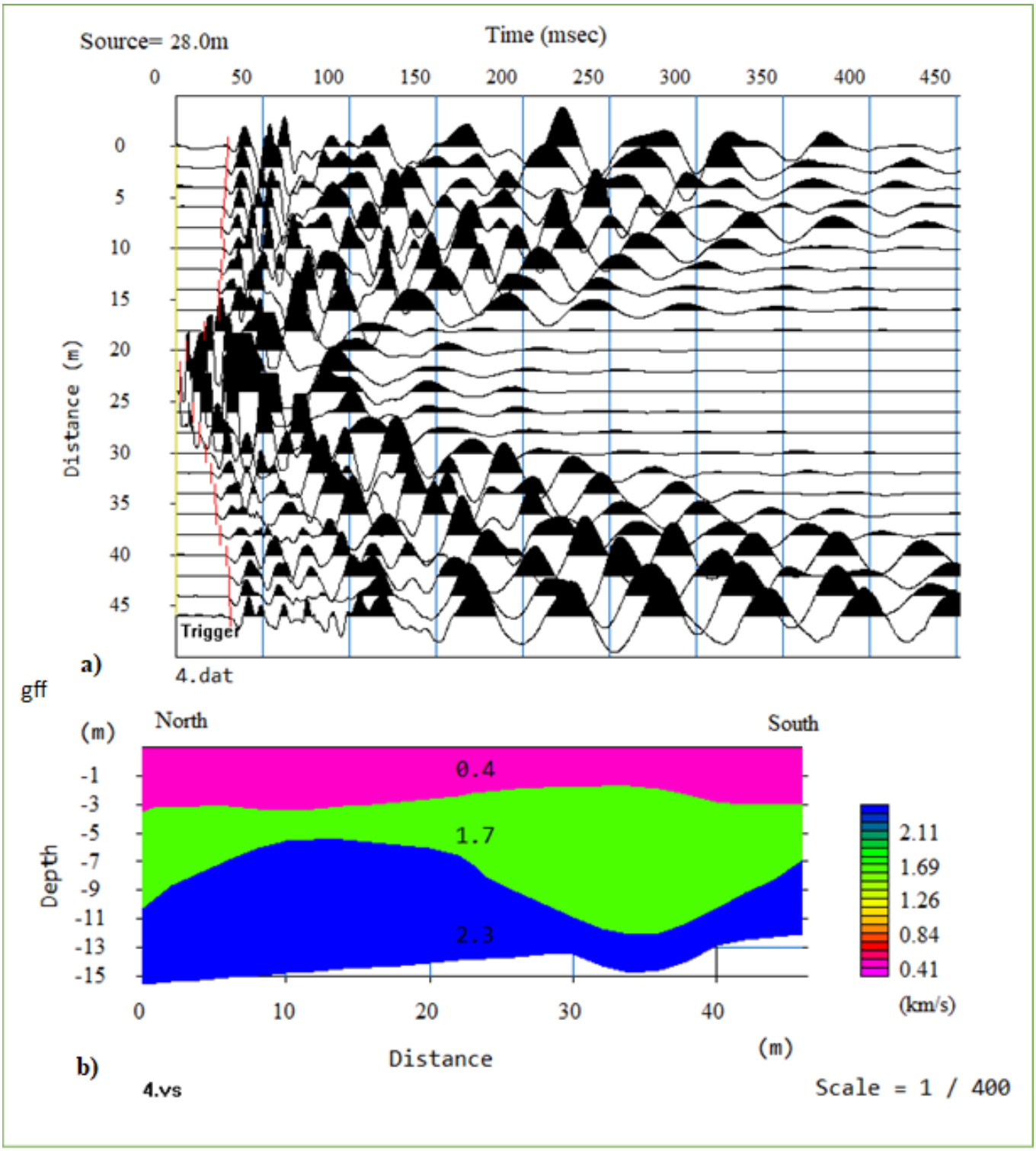

Figure4. 6: a) Wave form data and picked first break (red vertical lines) at the middle shot of Profile-1 and, b) time –term velocity model for the same profile.

CHAPTER FIVE

RESULT, DISCUSSION AND INTERPRETATION

5.1 Introduction

To conduct reliable interpretation and obtain clear picture about the foundation conditions of this specific site, integrating all the geophysical survey data collected from the site and comparing the results with secondary geological information from nearby boreholes is proper. The interpretation of individual 2D electrical tomography, Vertical Electrical Sounding data points and seismic refraction survey results are presented in the form sections, plan maps and individual sounding curves. Interpretation and analyses of the geo-electric section and compressional wave velocity models are made and compared with the result of available lithological borehole log data from nearby areas, and through this attempt, it is expected to minimize possible data interpretation ambiguities.

For this study, the depth of the boreholes used for lithological correlation is 10m; whereas the depths of the electrical tomography sections are about 9.18m, the VES method has mapped the subsurface to about 37m depth whereas the seismic refraction technique is seen to have mapped from 11-15m depth, i.e. In general, the depth of the geotechnical boreholes is relatively smaller as compared to the depth of the electrical sections.

5.2 Electrical resistivity survey

To understand both the lateral and vertical variations within the underlying formations that serve as foundation materials for engineering structures the combination of ERT and VES surveys that were applied and their results are explained below.

5.2.1. Vertical Electrical Sounding (VES)

As detailed in previous sections, the VES data were collected from four stations distributed over the available clearing very close to the study site that would allow adequate linear space (requirement for the VES survey) and are distributed on one traverse. The spacing between each VES station and the maximum current electrode spacing (AB/2) max are 50m and 220m respectively. The VES data are displayed in the form of pseudo-depth and geo-electric sections so as to facilitate their interpretation.

Figure 5.1 gives the pseudo-depth section plot which displays the resistivity distribution both vertical and laterally. This is a simple plot of the undisturbed raw VES data as a function of (AB/2) max. It has relatively a simple feature that reflects four distinct anomaly (sections) with contrasting responses and gradually

increasing with depth. Accordingly, the uppermost section is characterized by low apparent resistivity values ranging from about 5 to 30Ω-m, which is associated with the response of top soil, composed of black, soft and highly plastic silty clay soil (black cotton soil) when it is compared with the borehole data. Its thickness appears greater at the center (in the region of VES-2) and is minimum around VES-4, which may show the variation in degree of weathering of the underlying units along the profile.

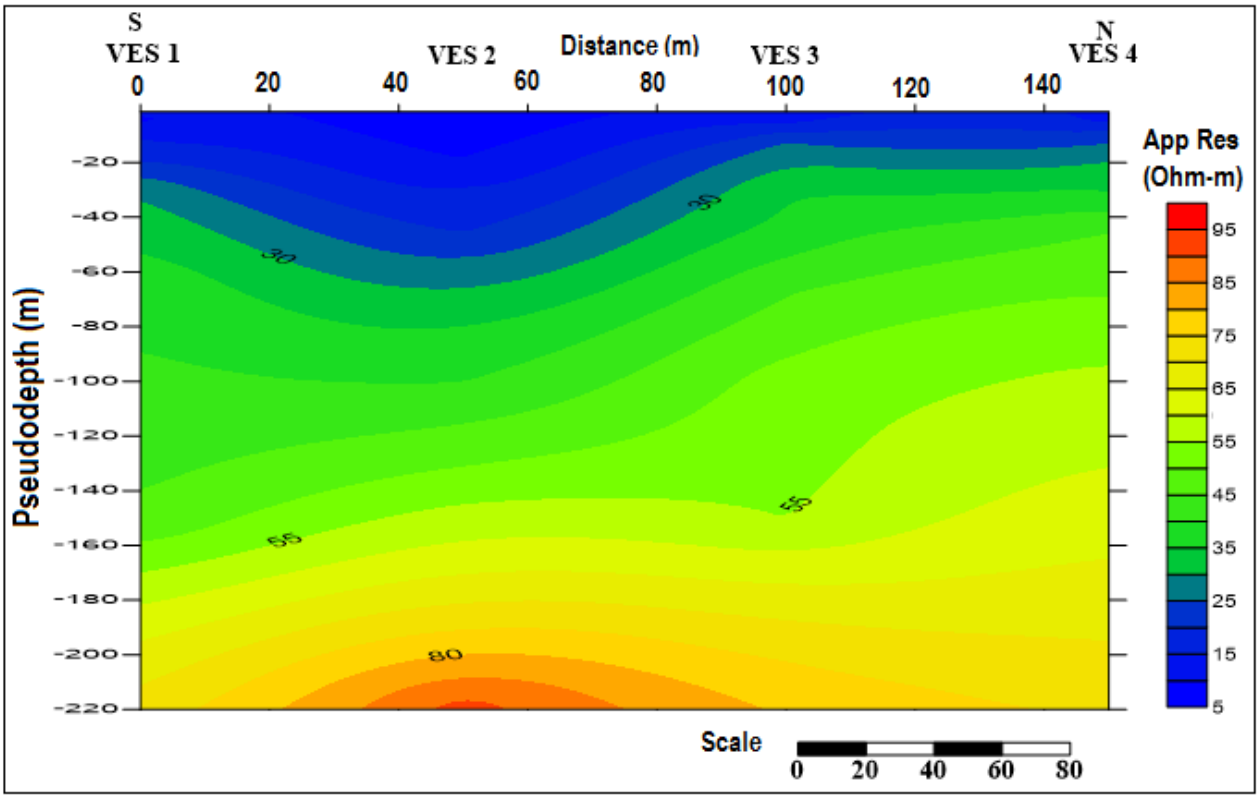

Figure 5. 1: The apparent resistivity pseudo-section along VES Profile.

Under the low resistivity section, there is an increment in resistivity valves to 30-55 Ωm which is corresponding to light gray, firm to very stiff, medium to high plastic clay and its thickness slightly increased in the region of VES 2 and VES 1 as compared to the other two VES stations. The third horizon has resistivity values varying from 55-80 Ωm and it is related to the response of the moderately to highly weathered ignimbrite rock. This section is slightly inclined from N to S. The bottom part of this profile is more observed at VES 2 and it is characterized by relatively resistive layer with values ranging from 80 to 100 Ω-m, which is related to moderately weathered bed rock.

On the other hand, the geo-electric section produced from the interpreted curve of the VES, oriented in a near S-N direction and providing quantitative subsurface information is shown in Figure 5.2. The first layer in the

section revealed a resistivity range of 5-7 Ω-m, which is due to the top black cotton soil. As can be observed on the geo-electric section (Figure 5.2), a low resistivity horizon is detected as a second layer beneath all sounding stations and this is due to the highly moisturized nature of the clay soil and its thickness is found to vary from 1.7 to 5.7m. Especially beneath VES station 2 it shows a higher depth or the fractured unit thickness reaches about 5.7m.

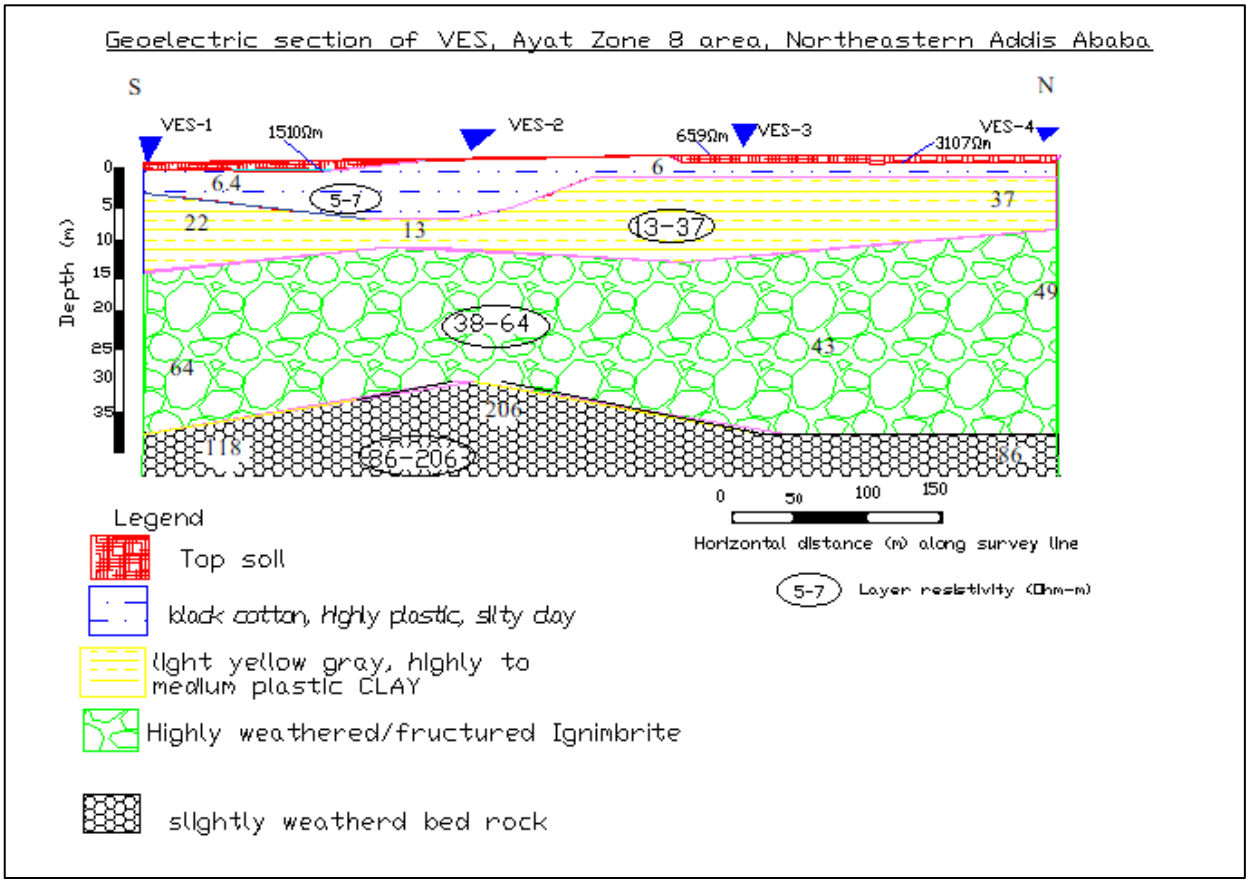

Figure 5. 2: Geo-electric section of the VES profile, Ayat Zone 8, Northeastern Addis Ababa.

The second layer is mapped by relatively small increase in its resistivity range (13-37Ω-m) and considerable thickness variation- thin at the North and meddle part of the profile (VES-2 and VES -4) and thicker 10.8m at south part of the profile (beneath VES-3 and VES-1). At the bottom of the top soil layer two geo-electric layers are interpreted as light gray, firm to stiff, medium to high plastic clay distinguished by relatively high resistive values ranging from 13 to 37Ω-m.

Generally, along the profile the resistivity values gradually increase with depth from a minimum of 5 Ω-m to a maximum of 206 Ω-m. Particularly, the third and fourth layers, interpreted as the responses of slightly

to moderate weathered ignimbrite, despite occurring at greater depth appear to be competent enough to be used as structural foundation.

5.2.1 Electrical Resistivity Tomography (ERT)

In addition to the sounding survey, axial dipole-dipole profiling was conducted along four profiles to better understand and identify the subsurface geo-electric layers underlying the target area and also examine the presence of vertical, near vertical structures and subsurface discontinuities detrimental to engineering foundation structures. Accordingly, the results of this survey are presented in form of 2D resistivity model sections and sliced stacked apparent resistivity maps and are discussed in the sections below.

5.2.1.1 ERT (along Profile 1)

The 2D resistivity data acquired employing the axial dipole-dipole configuration with a maximum electrode spacing of 5m and six (n=1, 2 . . . 6) dipole levels were processed using the Res2Dinv software. The total length of this profile is 130m and the inversion shows the clear and quality data with the RMS errors of 15.3 % after 3 iterations. The resulting inverse model resistivity section for this profile is shown in Figure 5.3.

The model actually describes the depth wise variation of low to high resistivity zones (2.72–122 Ωm) while the thin top soil whose thickness may cover the first 0.8m cannot be fully reflected on the ERT model. From the presented 2D model, at least, two sections can be identified that can be correlated with distinct lithological features observed from nearby borehole log data. Accordingly, the first section shows low resistivity and it corresponds to the black cotton soil (highly plastic clay and silty clay). The thickness of this section increases from south to north (0.85m to 4.62m) and also, as presented in data acquisition in Chapter four, this profile line data collected at the front of a rising buildings after 90m distance shows very low resistivity as compared with the previous distance until 9.18m. This low resistivity section may represent the deposited soil for filling the excavated soil during constructing the two high rise buildings. Due to this the region holds moisture and rain dropped from the buildings and saturating the soil horizon. The second layer has increased resistivity response as compared with the first and it may be the response of the highly to moderate weathered bed rock with the depth reaching to 9.18m and along this section, specifically at 50m distance of the profile shows a vertical discontinuity that may be interpreted as a hidden drainage pathway or vertical fracture in the rock units.

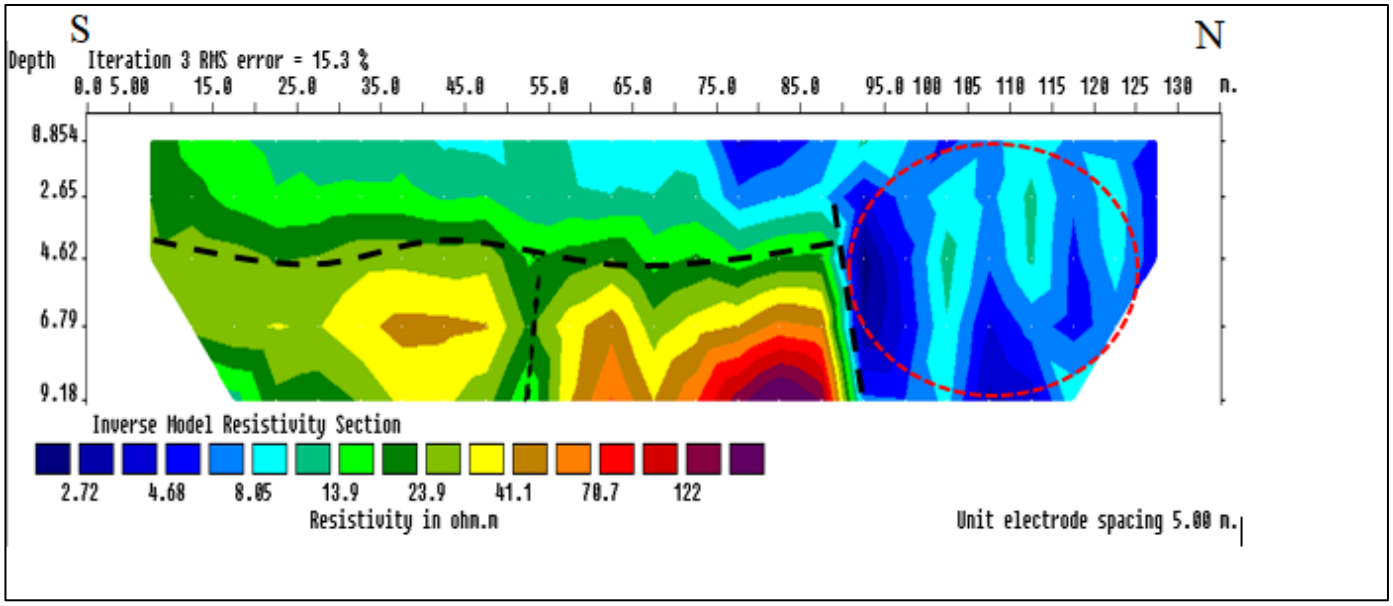

Figure 5. 3: 2D resistivity model section along ERT-1.

5.2.1.2 ERT (along Profile 2)

ERT2 (Profile 2) runs parallel to the first profile at the back side of the two high rise buildings and is about 30m from the first profile. The total length of this profile is 125m and the inversion result shows data with the RMS errors of 14.5 % after 3 iterations. The resulting inverse model for this profile is shown in Figure 5.4.

The model actually describes the depth wise variation of low to high resistivity zones (3.44–63 Ωm) corresponding to black cotton soil as the first horizon. Profile 2 is relatively similar with the first profile as both 2D models show two sections but in this profile the first layer resistivity and depth are similar until the final portion of the profile length. The depth of the first layer is about 3m and, in the region of 40m and 90m distance, the model shows discontinuities that may be interpreted as fractures in the bedrock. The bottom portion of the inverse model section shows the weathered bed rock, continuous in the region of 45m to75m of the profile distance where the bedrock starts from 6.79m depth which is related to the response of light gray, slightly to moderate weathered, weak to medium strong ignimbrite when correlated with the lithologic log. The two-three near vertical structures within the bedrock located at 30m, 70m and 90 m along the profile need special consideration during foundation design.

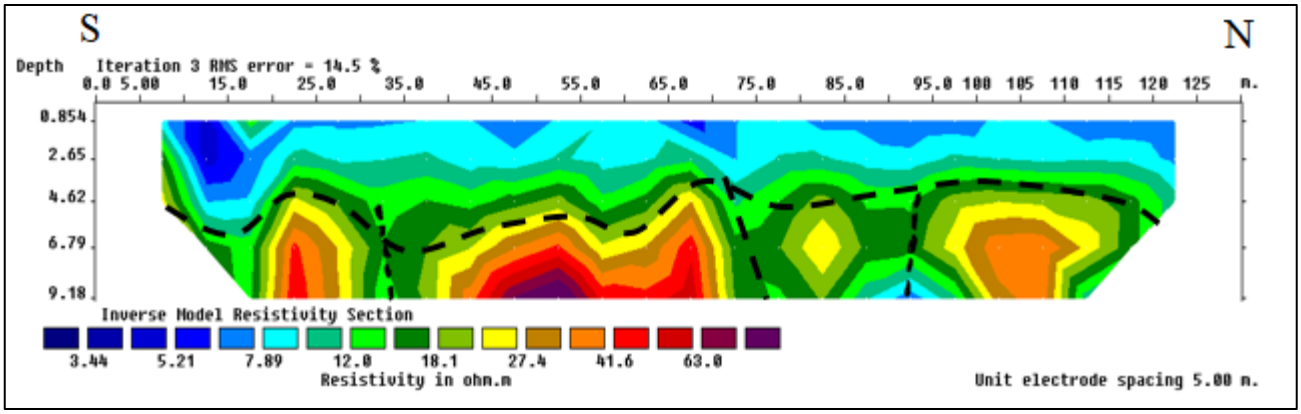

Figure 5. 4: 2D resistivity model section along ERT-2.

5.2.1.3 ERT (along Profile 3)

Profile 3 is slightly diagonal to both profiles one and two and is oriented from SW to NE. The total length of this profile is 90m and the inversion result shows the data with the RMS errors of 15.9 % after 3 iterations. The resulting inverse model resistivity section for this profile is shown in Figure 5.5.

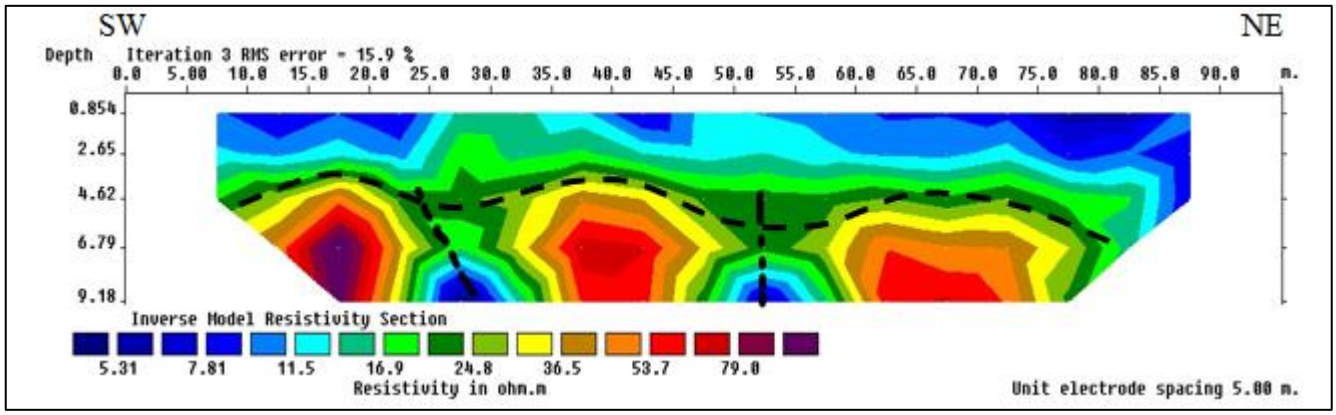

Figure 5. 5: 2D resistivity model section along ERT-3.

This profile could be again be classified into two different section in agreement with the geological information from borehole data. Along the profile, the resistivity values of the top layer are very low and vary from 5.31 to 16.9 Ω m and these resistivity responses are that of the black, high plastic silty clay top soil. The depth of the first section is seen to vary from 2.65 to 4.62m from S to N. The 2D electrical resistivity section obtained on this line is characterized by a high degree of fracturing extending to depth at 25m and 50m distance of the profile to the investigated depth of 9.18m. Near vertical weak zones around 25 and 55m along the profile are noteworthy.

5.2.1.4 ERT (along Profile 4)

The fourth profile is perpendicular to the first two profiles around and 70m distance of them oriented from west to east while the topography of study area is slightly inclined from west to east. The total length of this profile is 105m and the inversion shows the clear and quality data with the RMS errors of 8.1% after 3 iterations. The resulting inverse model resistivity section for this profile is shown in Figure 5.6.

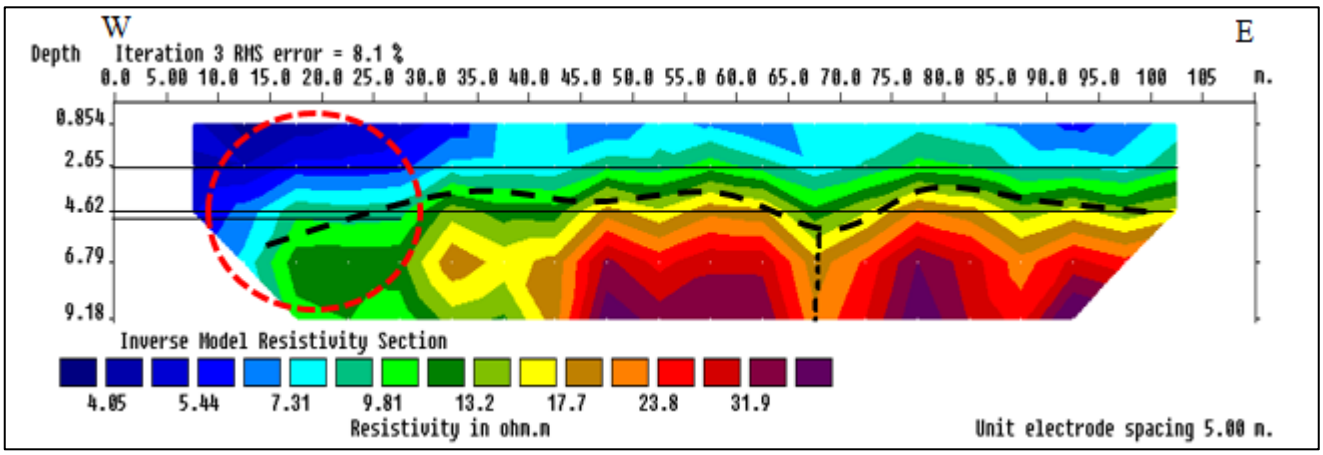

Figure 5. 6: 2D resistivity model section along ERT-4.

Around the beginning of this profile there are condominium buildings and a garbage ditch. The profile could be classified in three sections after some distance from its beginning, but up to 45m it has two section. The first section shows low resistivity as compared with the others section and varies from 4.05 to 9.81 Ω m with the depth of 4.62m and it corresponds to the black cotton soil saturated with moisture and the unit may be debris from excavations during the condominium construction and deposited there (region marked with circle). The second section is seen to gradually increase in resistivity from the top layer which varies from 9.81 to 17.7 Ω m with 2.65m to 4.62m depth variation, but in the first 45m distance of the profile, the top layer depth goes to 4.62m and the second section reaches 9.18m depth.

After 45m distance of the profile, it has the third horizon having high resistivity than the top layers and varies 17.7 to 31.9Ω m. At 70m distance, the profile shows a zone which could be interpreted as a weak zone or a fracture in the bedrock. When this section is compared with the borehole data, it correlate with light gray, slightly to moderate weathered, weak to medium strong ignimbrite.

5.2.3 Combination of the 2D electrical resistivity tomography profiles

The stacked apparent resistivity ERT section map (Figure 5.7) shows the sub-surface resistivity section of the entire study area which was constructed by extracting apparent resistivity values of the first three profiles for the same depth of investigation. In order to obtain a more reliable representation of the possible subsurface stratification, four depth slices (for 2.1m, 4.8m, 6.1m, and 8.7m depths) were selected from the electrical resistivity tomography data to characterize the subsurface.

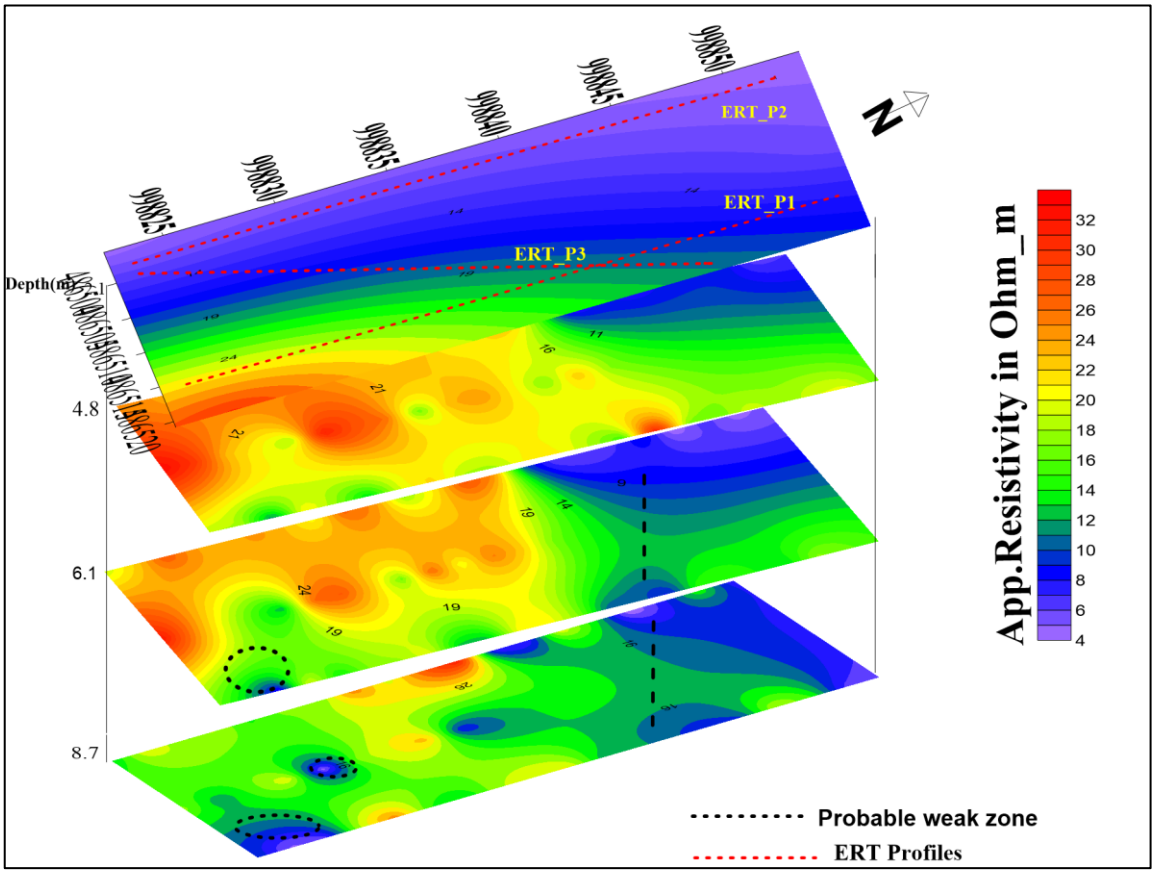

Figure 5. 7: Stacked apparent resistivity map of the ERT data.

The resistivity of the study area are seen to gradationally decrease towards the northern direction. Relatively higher resistivity responses of the weathered to fresh bedrocks is observed at shallow depths near the south side of the survey area. As one can see from the Figure 5.7 the fractured regions follow from NW to SE direction in the survey area with its depth reaching and continuing from 8.7m. Based on the stacked apparent resistivity map of the ERT data, the region at the beginning of the survey shows probable weak zones or fractured zones trending slightly from NW to SE direction. When one compares this stacked apparent resistivity map of the ERT with the VES profile, the weak zones are seen to continue in the region of VES2.

5.3 Seismic refraction survey

The seismic refraction data were acquired over two profiles with 2m geophones spacing and 5m near forward and reverse shot and a number of mid line shot points. The data were processed using PICKWIN*ver.4.0.0.4 2008* and Plotfera_ee ver.2.9.1.2 software. The interpretation of these seismic refraction data are displayed in the form of velocity models and are as discussed below.

5.3.1 Velocity model for profile_1

This profile runs parallel to the first two profile of the ERT line and a 24 channel seismic refraction spread with 5m beyond shot, i.e., having a total length of 48m was acquired. Its velocity model is illustrated in Figure 5.8 which shows three distinct layers with P-wave velocity changing from 0.4 to 2.4 km/s.

The upper layer is characterized by low compressional wave velocities ranging from 0.4 to 0.42 km/s and its thickness approximately varying from 2.5-3.5m. This low velocity is due to the top black cotton and silty clay soils, while the second layer, which is marked by comparatively intermediate P-wave velocity that varies from 1.36 to 1.79km/s is associated with the response of light gray, medium to high plastic clay undulated morphology the thickness of this layer is maximum (12m) at the south side around 35m from north in the profile and at the center around 10m from north to south in the profile is 3m thick. The bottom layer, which is marked by comparatively high P-wave velocity that varies from 2.2 to 2.4km/s is associated with the response of the moderately weathered ignimbrite showing also undulating morphology which seem to be deeper at the center of the profile (9m), which is around 40m distance from south to north in the profile and thinner in the south direction of the profile which is almost 3m depth.

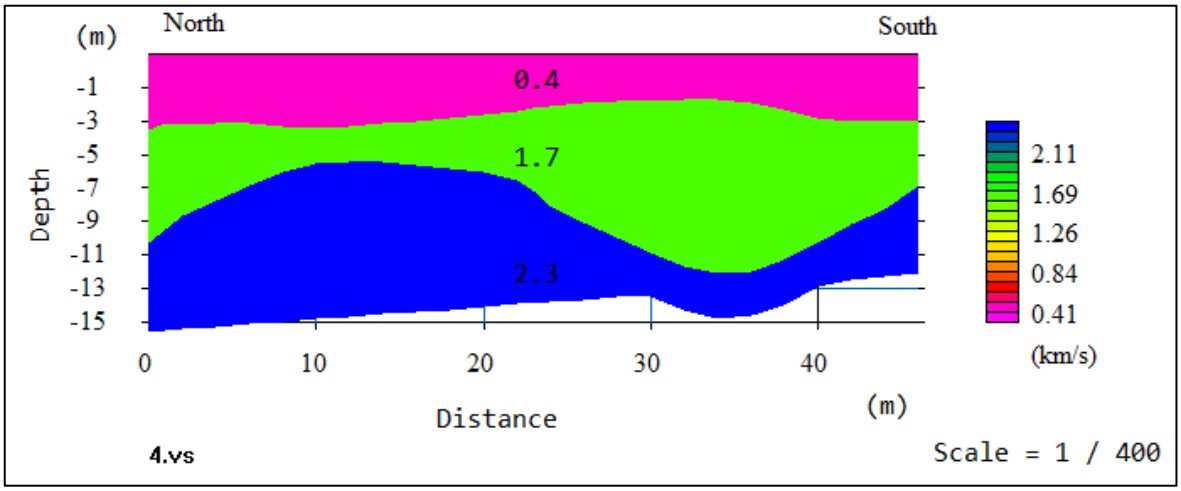

Figure 5. 8: Velocity model along Profile_1.

5.3.2 Velocity model for Profile_2

This profile is 48m long with beyond shot 5m and its velocity model is displayed in Figure 5.9. It shows three layers differentiated with contrasting P-wave velocities, ranging from 0.29 to 1.99km/s. The first layer has indicated low compressional wave velocity varying from 0.29 to 0.3km/s and 2-3m thickness, which is due to the upper dark clay-silty clay soil. There is slight difference between the two underlining layers velocity model and they are shown to be undulating. The second layer has P-wave velocity varying between 1.7-1.81 km/s with 4-7m thickness variation, which is deeper at 10m and 40m on the SE to NW distance of the profile. This response is due to the light yellow, medium plastic sandy clay and silt. P-wave velocity of the third layer is seen to vary from 1.81-1.99 km/s with variation in depth and thickness (4-13m) and this is believed to be due to the moderately weathered light to dark gray ignimbrite forming the bedrock in the area.

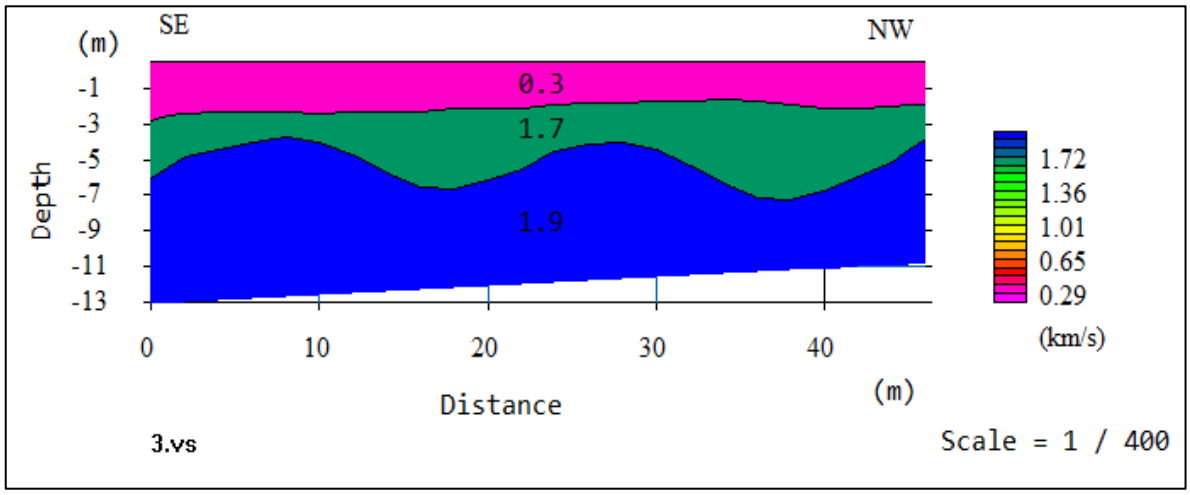

Figure 5. 9: Velocity model along seismic Profile-2.

5.4. Integrated geophysical and geological data analysis

5.4.1 Analysis of 2D ERT models and VES geo-electrical sections

The integration of geophysical methods resolves the subsurface layers more and give definitive and unambiguous result rather than using any individual method. In order to achieve this, analyses of ERT models and VES geo-electrical sections are integrated to better determine the individual subsurface layers of the study area. From general point of view, the axial dipole -dipole profiling is more reliable at delineating the subsurface morphologies clearly (both lateral and vertical resistivity contrast). However, the vertical electrical sounding shows the layer resistivity directly below the sounding point and general resistivity distribution of target site.

5.4.1.1 ERT-Profiles-2 and VES profile

Figure 5.10 demonstrates the correlation between the Vertical Electrical Sounding and the nearest Dipole-Dipole electrical resistivity tomography profiling (ERT_p2) survey results, which revealed almost identical trends about the subsurface characteristics. Both results confirm that the resistivity is increasing with depth and they also show the competency of the formations increases with increasing depth. In addition to this, in both sections the weak zones and /or near vertical structures or fractures are seen to trend the direction of NW to SE.

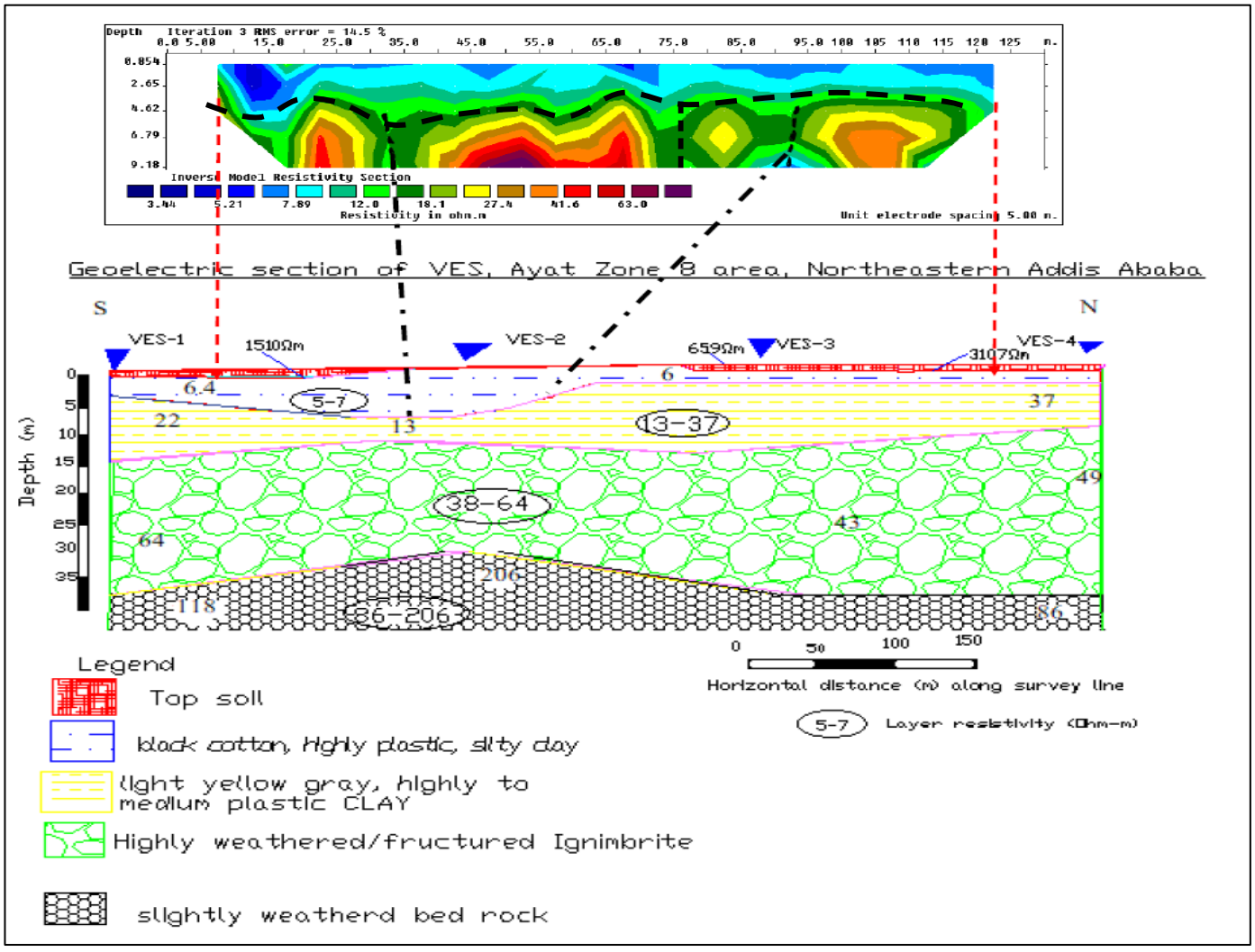

Figure 5. 10: Correlation of the ERT result of Profile-2 versus geo-electrical section of VES profile.

5.4.2 Analysis of seismic refraction Profile-2 and VES geo-electrical section

As demonstrated in Figure 5.11 the correlation between the seismic refraction and VES geo-electrical survey results reveal almost identical trends about the subsurface characteristics. Both results confirm that the P-

wave velocity and resistivity are increasing with depth, it further shows that the competency of the formations increases with increasing depth. In addition to this, in both sections the weak zones and /or near vertical structures or fractures are seen.

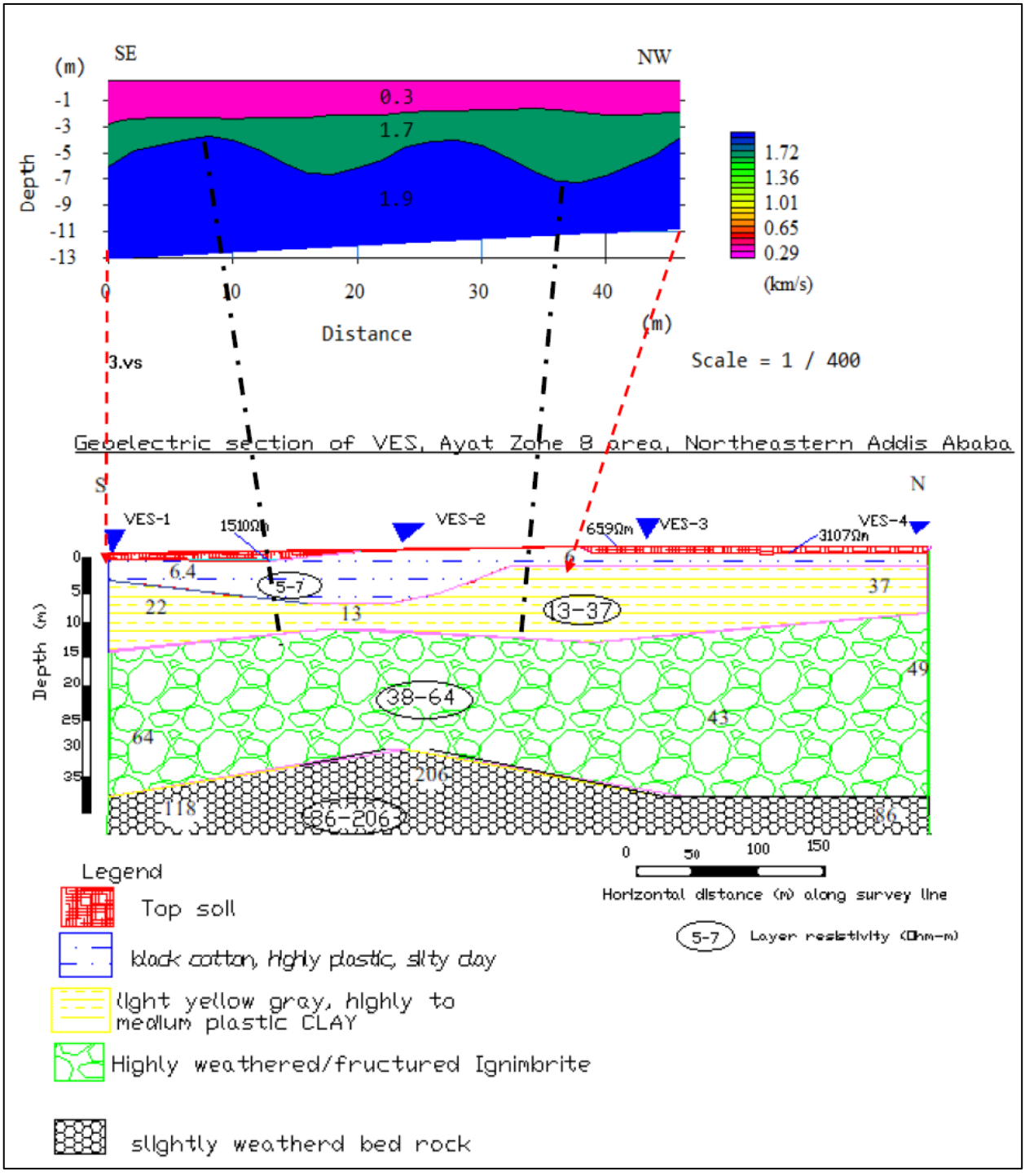

Figure 5. 11: Correlation of the seismic refraction Profile-2 versus geo-electrical section of the VES profile.

CHAPTER SIX
CONCLUSIONS AND RECOMMENDATIONS

6.1 General

An integrated study involving a number of geophysical investigation techniques and geotechnical log data were carried out at the construction site of the Ayat real estate located in YekaAyat condominium area, Northeast of Addis Ababa. The geophysical surveys included electrical resistivity sounding (VES), axial dipole-dipole profiling and seismic refraction surveys. A lithologic log data of a nearby borehole was also used to calibrate the results of the geophysical survey and constrain the results. Analyses of these data were conducted with the purpose of mapping the subsurface geology and describe its suitability for the construction of multistory residential and commercial complexes. In this Chapter we present the summary of this work and give some concluding remarks about the work. A final section gives some recommendations for the foundation work being currently undertaken based of those results.

6.2 Conclusions

From the integration of the surveying results and available lithological log data around the study area the following conclusions are drawn:

i. From 2D resistivity models, geo-electric section of VES and seismic velocity model two to four distinct subsurface layering are identified that are associated with different lithological units. The top layer is characterized by low resistivity (3.03-8Ω-m) and low P-wave velocity less than 0.42 km/s and is associated with the effect of the upper black cotton soil, composed of highly plastic clay and silty clay materials. The thickness of the layer varies from 1.6m to 5.7m. Underlying the top layer, there is relatively thicker unit than the first layer, with its depth is varying from 1.6m-12.3m, its resistivity varying from 13-37Ω-m and medium P-wave velocity (<1.79km/s) response which is attributed to the light gray, medium to highly plastic clay, which is found to be inclined from north to south direction of the study area. From the 2D resistivity models, geo-electric section of the VES and seismic velocity models, the third layer is found to be the response of slight to moderately weathered ignimbrite. This layer represents the bedrock in the study area and is characterized by increment of depth (varying from 12.3m to 37.6m) from north to south direction of the study area with undulating morphology. Its resistivity is found to vary from 38 to

65Ω-m and P-wave velocity is less than 2.4km/s. On the other hand the bottom layer mapped with the survey is a fresh to slightly weathered bed rock, which is clearly observed under the first 20-60m distances of the study area from north to south direction and its resistivity is found to vary from 86 to 206Ω-m. Based on the result of ERT profiles and the VES profile, around 50m and 70m distances on the survey lines and at various locations over the profiles and over the study area in general, a number of near vertical fractures identified as weak zones and fractures oriented in a direction from NW to SE are mapped. All these subsurface discontinuities are believed to be detrimental in foundation design work of large structures and need to be given due consideration. At places the depth to the surface of the competent hard formation for foundation is found to reaches up to 12m.

ii. The gradual increasing of resistivity and P-wave velocity responses with depth is a direct indication of continuous change of engineering properties of the subsurface formations, and due to this, it provides a hint for the increasing competency of the foundation materials with depth.

iii. The low resistivity determined for shallow depths ranged and fracture parts determine the physically weak nature of the top black cotton soil, silty clay and deposit soil, which are not preferred foundation materials.

iv. The resistivity of the layers is found to increase with depth and relatively the region of VES 2 (possibly a fill in debris material) is of low resistivity in the second layer, due to this, groundwater may easily percolate down into the deeper formations and generally no effect of shallow groundwater on the foundations is expected.

6.3 Recommendations

Based on the outcomes of this study, the following recommendations are made in relation to the foundation work being currently undertaken in the area:

- The upper section of the site mainly consisted of black cotton and silty clay soils are not competent enough to bear loads from heavy engineering structures. Therefore, erecting structures over such relatively weak formation require proper engineering measures during the design and construction stages. Hence, in addition to other precautionary measures, compaction, stabilization, removing and backfilling by another well graded material can be implemented as supplementary remedial steps.

- To prevent percolation of surface runoff to soil and thereby protect the base of the structures from cracking and settlement, proper drainage should be constructed to maintain the moisture content in the underlying materials.
- As the study area is close to the Main Ethiopian Rift (MER), a system of weak zones and undesirable soil for construction amplify and aggravate earthquake effects, the likely impacts of seismic activity should be considered carefully during designing and construction of multistory buildings.
- To better refine and confirm the geophysical results over the wide area of the construction site, further geotechnical drilling work is essential and recommended: especially in regions where the thickness of the black cotton soil is maximum and minimum.

References

Araffa, S. A., Mohamadin, M. I., Saleh Sabet, H., and Takey, M. S. (2019). Geophysical interpretation for groundwater exploration around Hurghada area, Egypt. NRIAG *Journal of Astronomy and Geophysics*, **8**(1): 171-179.

Aseged Getahun (2007). Geology of Addis Ababa City. Unpublished Report. Addis Ababa: Office of the Ministry of Mines and Energy Regional Geology and Geochemistry Department, Addis Ababa, Ethiopia. pp 36.

Atalay Ayele (2005). History and operational capability of the Ethiopian Seismic Station Network (ESSN). SINET: *Ethiopian Journal of Science*, **28**(1): 93-98.

Barker, R.D., (1999). Surface and borehole geophysics. In Lloyd J. W. (ed) Water Resources of Hard Rock Aquifers in Arid and Semi-Arid Zones. *Studies and Reports in hydrology*, 58, Paris, UNESCO, pp 287.

Belete Getahun (2018, June). Integrated Geophysical Characterization for Building Foundation at Kilinto, Akaki Kality Sub-City, Addis Ababa, Central Ethiopia. Unpublished MSc thesis.pp 90.

Benson, R. C. (1993). Geophysical techniques for subsurface site characterization. *Geotechnical Practice for Waste Disposal*, pp 311.

Challoner, R. (1847). The Holy Bible, translated from the latin Vulgate, diligently compared with The Hebrew, Greek, and other Editions, in divers languages: The Old Testament Douay;# a. D. 1609. And the New Testament Rheinis, a. D. 1582. With annotations by the Rev. Challoner.. (Vol. 2). Richardson and Son. pp 1602.

Cousin, I., Samouëlian, A., Tabbagh, A., Bruand, A., and Richard, G. (2005). Electrical resistivity survey in soil science: a review. *Soil and Tillage research*, **83**(2): 173-193.

Engida Zemedagegnehu (2001). Groundwater Study of Addis Ababa Area. Report No. 01/93.pp 29.

Eyasu Leta (2014). Application of integrated geophysical techniques to map deep groundwater potential zones and geological structures at south-west Akaki, south-east of Addis Ababa, Ethiopia. Unpublished MSc thesis. pp 117.

Fkirin, M. A., and Badawy, S. El deery MF (2016). Seismic refraction method to study subsoil structure. *J Geol Geophys*, **5**(259):5.

Gouin, P. (1979). Earthquake history of Ethiopia and the Horn of Africa. IDRC, Ottawa, ON, CA. pp 5-9.

Hailemariam Siyoum (2011).Integrated geophysical and direct geotechnical investigations for building foundation at addis ababa science and technology university, Akaki, Addis Ababa, Ethiopia. Unpublished MSc thesis. pp 100.

Haile Selassie Girmay, Getaneh Assefa (1989). The Addis Ababa-Nazareth Volcanism: A Miocene-Pleistocene V geophysical techniques to investigate the groundwater table at the Great Pyramids of Giza, Egypt. *Geoscientific Instrumentation, Methods and Data Systems*, **8**(1): 29-43.

Hassan, E., Rai, J. K., and Anekwe, U. O. (2017). Geoelectrical Survey of Groundwater in Some Parts of Kebbi State Nigeria, a Case Study of Federal Polytechnic Bye-Pass Birnin Kebbi and Magoro Primary Health Center Fakai Local Government. *Geosciences*, **7**(5): 141-149.

Kearey, P., Brooks, M., and Hill, I. (2002). An introduction to geophysical exploration. third edition.pp 281.

Kumar, N., Rao, R., and Naganjaneyulu, K. (2015). Electrical resistivity imaging (ERI) using multielectrodes for studying subsurface formations in Cauvery plains. Adv. App. Sci. Res, 6, 47-53.

Laskar, A., and Pal, S. K. (2012). Geotechnical characteristics of two different soils and their mixture and relationships between parameters. *EJGE*, **17**: 2821-2832.

Loke, M. (2000). Electrical imaging surveys for environmental and engineering studies: A Practical Guide to 2D & 3D Electrical Imaging Surveys. Technical Reports.pp 129.

Loke, M. (2004). Electrical imaging surveys for environmental and engineering studies: A Practical Guide to 2D & 3D Electrical Imaging Surveys. Technical Reports.pp 136.

Medhanit Akalu (2017). Engineering Characteristics of Red Soil: A Case from Western Addis Ababa, Ethiopia.unpublished MSc thesis.pp 100.

Messele Haile (2004). Seismic Microzonation for the city of Addis Ababa by using Microtremors. 13th World Conference on Earthquake Engineering. Vancouver, B.C., Canada.

Mulugeta Dadi, Diekkrüger, B., & Roehrig, J. (2016). Characterization of water level variability of the main Ethiopian rift valley lakes. *Hydrology*, **3**(1). pp 14.

Molla Demlie, Stefan Wohnlich, Birhanu Gizaw and Stichler W.(2007). Groundwater recharge in the Akaki catchment, central Ethiopia: evidence from environmental isotopes (d18O, d2H and 3H) and chloride mass balance. Published online 12 October 2006 in Wiley InterScience. *Hydrol. Process.* **21**:807–818.

Morton, W.H. (1979). Riftward Younging of Volcanic Rocks in the Addis Ababa Region. Rift Valley Ethiopian. *Nature,* **280**(5720): 284-288.

Niculescu, B. M. (2018). Forward modeling of vertical electrical soundings with applications in the study of sea water intrusions. International Multidisciplinary Scientific GeoConference: SGEM: *Surveying Geology & mining Ecology Management,* **18**: 803-810.

Octova, A., and Yulhendra, D. (2017). Iron ore deposits model using geoelectrical resistivity method with dipole-dipole array. In MATEC Web of Conferences EDP Sciences **101:** 04017.pp 6.

Olayanju GM, Mogaji KA, Lim HS and Ojo TS (2017). Foundation integrity assessment using integrated geophysical and geotechnical techniques: Case study in crystalline basement complex, southwestern Nigeria. *J Geophys Eng,* **14**: 675- 690.

Oyediran, I. A., and Falae, P. O. (2018). Integrated Geophysical and Geotechnical Methods for Pre-Foundation Investigations. *J Geol Geophys,* **8**:1. pp 9.

Perrone, A., Lapenna, V., and Piscitelli, S. (2014). Electrical resistivity tomography technique for landslide investigation: a review. *Earth-Science Reviews,* **135**: 65-82.

Redpath, B. B. (1973). Technical Report E-73-4: Seismic Refraction Exploration for Engineering Site Investigations. National Technical Information Service. pp 70.

Samouelian, A., Cousin, I., Tabbagh, A., Bruand, A., & Richard, G. (2005). Electrical resistivity survey in soil science: a review. *Soil and Tillage research*, **83**(2): 173-193.

Selamawite Tadesse (2017). Building Foundation Characterization Analysis:A Case Study in Ayat Area, Bole Sub-City,Addis Ababa, Central Ethiopia. Unpublished report.pp 122.

Sharafeldin, S. M., Essa, K. S., Youssef, M. A., Karsli, H., Diab, Z. E., and Sayil, N. (2017). Shallow geophysical techniques to investigate the groundwater table at the Great Pyramids of Giza, Egypt. *Geoscientific Instrumentation, Methods and Data Systems,* **8**(1): 29-43.

Shendi, E. H. (2008). Electrical Prospecting Methods. Department of Geology, Faculty of Science, Suez Canal University Monograph.pp 128.

Soupios, P., Georgakopoulos, P., Papadopoulos, N., Saltas, V., Andreadakis, A., Vallianatos, F., Sarris, A. and Makris, J.P. (2007). Use of engineering geophysics to investigate a site for a building foundation. *Journal of Geophys-ics and Engineering,* **4**(1):94–103.

Tamiru Alemayehu (2001). The Impact of Uncontrolled Waste Disposal on surface water quality in Addis Ababa, Ethiopia.SINET:*Ethiop.J.Sci.***24**(1):93-104.

Tamiru Alemayehu, Tenalem Ayenew, Dagnachew Legese, Yirga Tadesse, Solomon Waltenigus and Nuri Mohamed (2006). Ground Water Vulnerability Mapping of the Addis Ababa Water Supply Aquifers. Unpublished technical report, Addis Ababa, Ethiopia.pp 80.

Tenalem Ayenew, Molla Demlie and StefanWohnlich (2008). Application of Numerical Modeling for Groundwater Flow System Analysis in the Akaki Catchment,centeral Ethiopia. *Math Geosci* (2008) 40: 887–906, DOI 10.1007/s11004-008-9144-x.

Tenalem Ayenew, Stefan Wohnlich, Molla Demlie (2008). Integrated Groundwater Modeling and Hydrochemical Study in Addis Ababa area: Towards Developing Decision Support System for Wellhead Protection. pp 1.

Tesfaye Asresahagne and Asmelash Abay (2016). Assessment and Evaluation of Volcanic Rocks Used as Construction Materials in the City of Addis Ababa. http://dx.doi.org/10.4314/mejs.v8i2.7.

Tigistu Haile and Alemayehu Ayele (2012). Environmental impact and vulnerability of the surface and ground water system from municipal solid waste disposal site: Koshe, Addis Ababa. *Environmental earth sciences*, **67**(1): 71-80.

Tigistu Haile and Alemayehu Ayele (2014). Electrical resistivity tomography and magnetic surveys: applications for building site characterization at gubre, wolkite university site, western Ethiopia. SINET: *Ethiop. J. Sci.,* **37**(1):13–30.

Tilahun Mommo (2005). Site-specific ground motion simulation and seismic response analysis at the proposed bridge sites within the city of Addis Ababa, *Ethiopia. Engineering Geology*, **79**(3-4):127-150.

Ugwu, G. Z., and Ezema, P. O. (2013). 2D Electrical Resistivity Imaging for the Investigation of the Subsurface Structures at the Proposed Site for Kauridan Estate at Ibagwa-Nike, Southeastern Nigeria. *International Journal of Scientific Research in Knowledge,* **1**(12): 528-534.

Appendix

Resist Graph

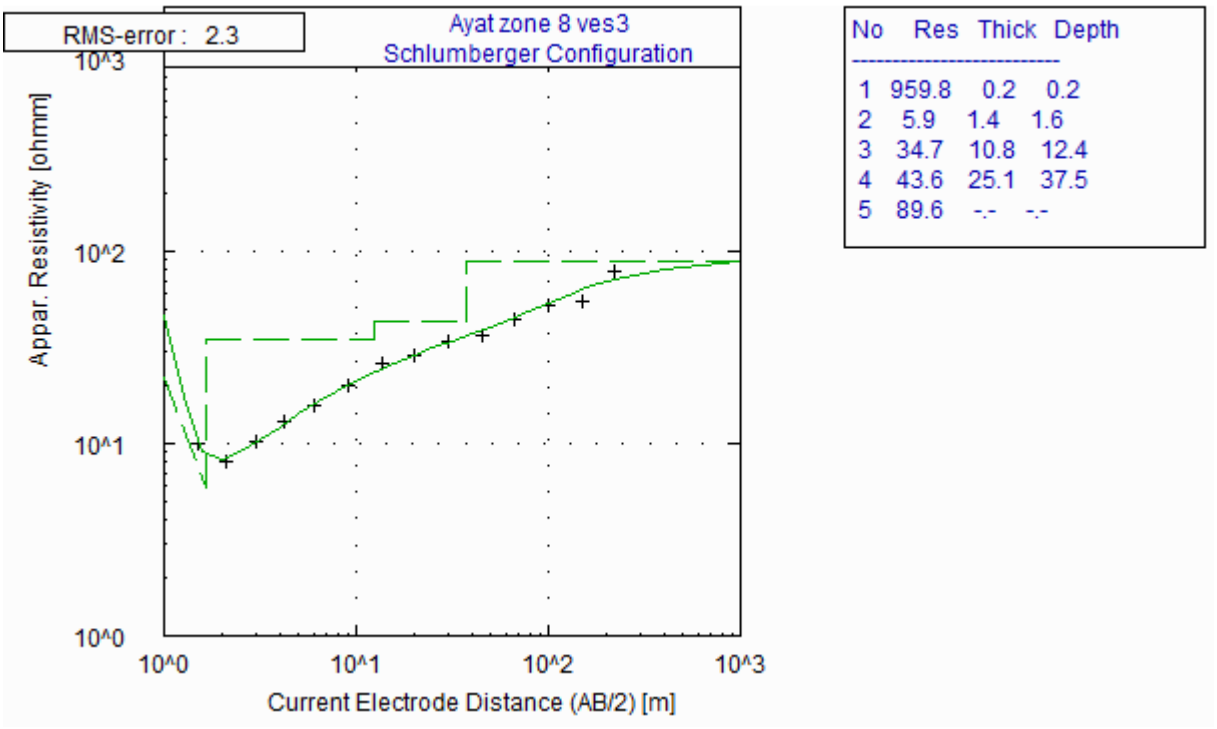

No	Res	Thick	Depth
1	959.8	0.2	0.2
2	5.9	1.4	1.6
3	34.7	10.8	12.4
4	43.6	25.1	37.5
5	89.6	-.-	-.-

Resist Graph

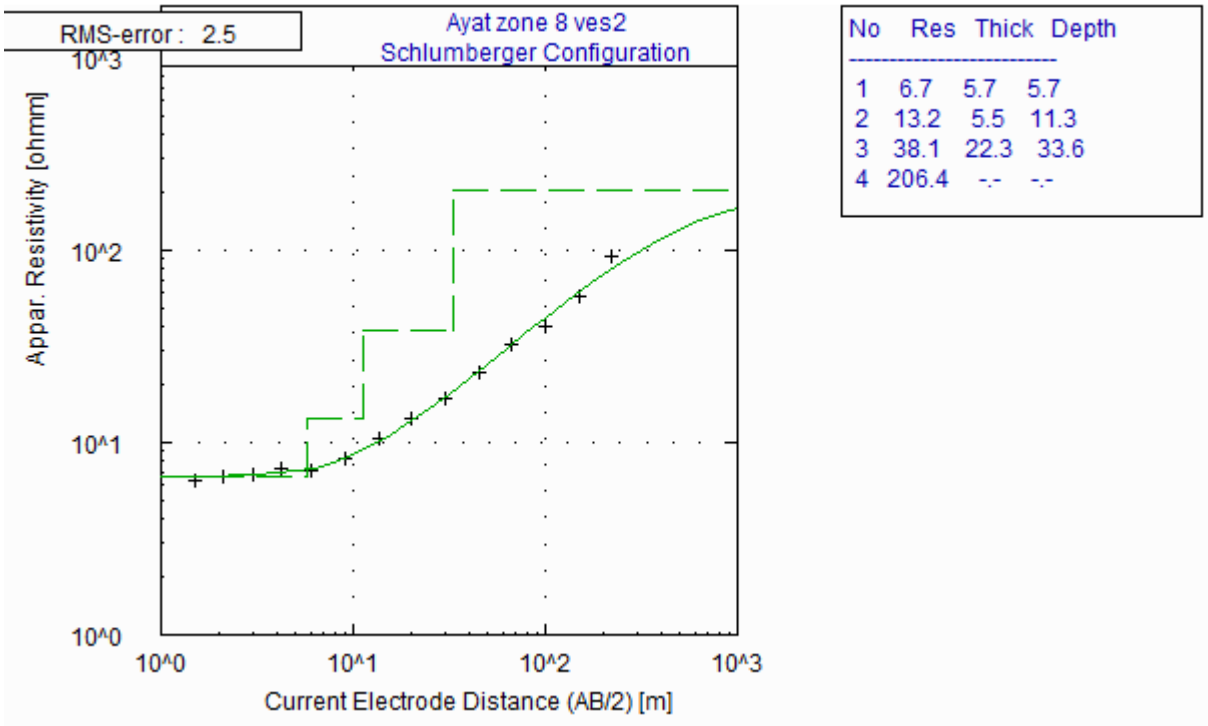

No	Res	Thick	Depth
1	6.7	5.7	5.7
2	13.2	5.5	11.3
3	38.1	22.3	33.6
4	206.4	-.-	-.-

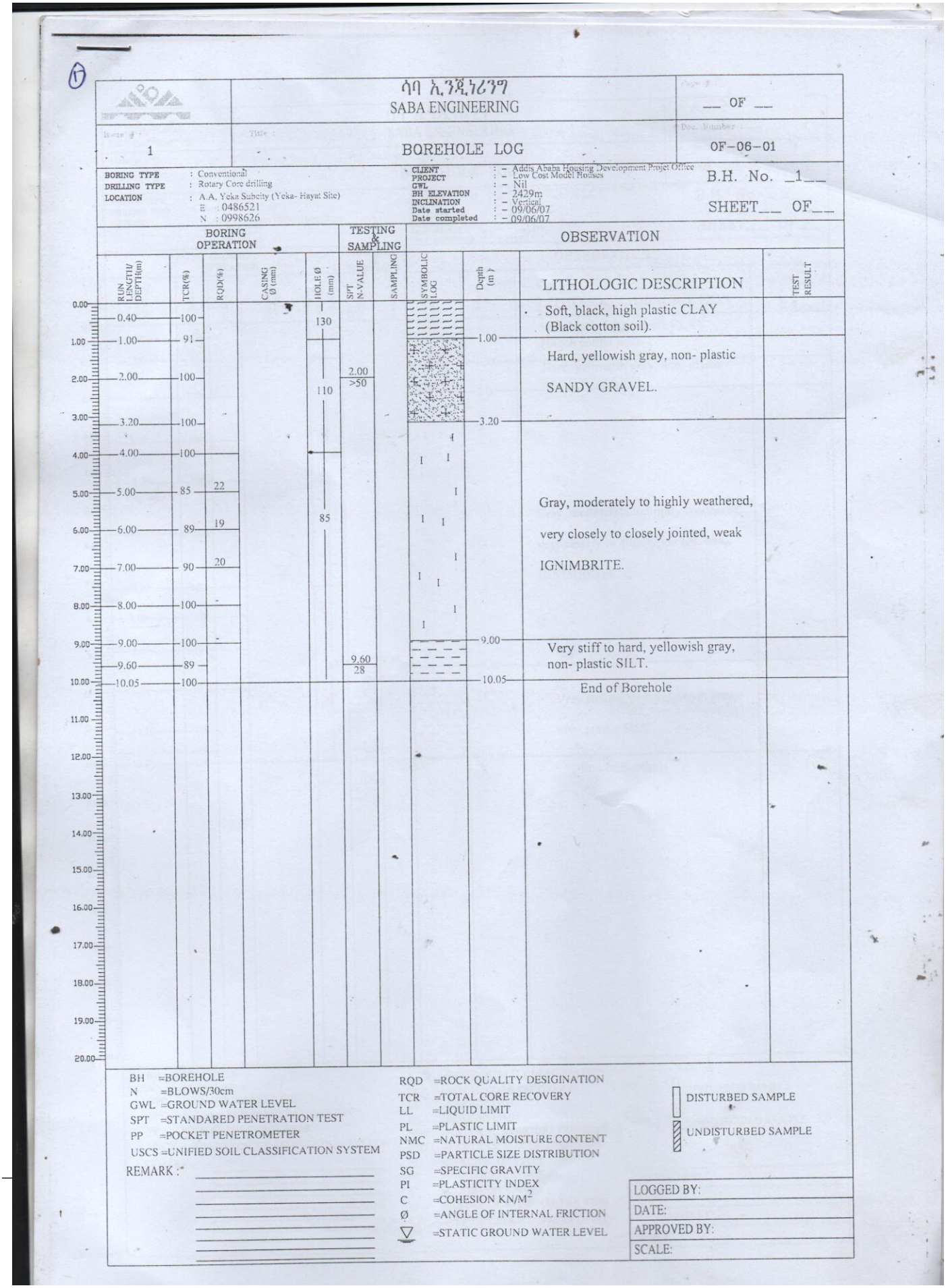

ሳባ ኢንጂነሪንግ
SABA ENGINEERING

__ OF __

Issue # : 1

Title : BOREHOLE LOG

Doc. Number : OF-06-01

BORING TYPE : Conventional
DRILLING TYPE : Rotary Core drilling
LOCATION : A.A, Yeka Subcity (Yeka- Hayat Site)
E : 0486521
N : 0998626

CLIENT : – Addis Ababa Housing Development Project Office
PROJECT : – Low Cost Model Houses
GWL : – Nil
BH ELEVATION : – 2429m
INCLINATION : – Vertical
Date started : – 09/06/07
Date completed : – 09/06/07

B.H. No. _1__

SHEET___ OF___

BORING OPERATION					TESTING & SAMPLING		OBSERVATION			
RUN LENGTH/ DEPTH(m)	TCR(%)	RQD(%)	CASING Ø (mm)	HOLE Ø (mm)	SPT N-VALUE	SAMPLING	SYMBOLIC LOG	Depth (m)	LITHOLOGIC DESCRIPTION	TEST RESULT
0.40	100			130					Soft, black, high plastic CLAY (Black cotton soil).	
1.00	91							1.00		
2.00	100			110	2.00 >50				Hard, yellowish gray, non- plastic SANDY GRAVEL.	
3.20	100							3.20		
4.00	100									
5.00	85	22							Gray, moderately to highly weathered, very closely to closely jointed, weak IGNIMBRITE.	
6.00	89	19		85						
7.00	90	20								
8.00	100									
9.00	100							9.00		
9.60	89				9.60 28				Very stiff to hard, yellowish gray, non- plastic SILT.	
10.05	100							10.05	End of Borehole	

BH =BOREHOLE
N =BLOWS/30cm
GWL =GROUND WATER LEVEL
SPT =STANDARED PENETRATION TEST
PP =POCKET PENETROMETER
USCS =UNIFIED SOIL CLASSIFICATION SYSTEM

RQD =ROCK QUALITY DESIGNATION
TCR =TOTAL CORE RECOVERY
LL =LIQUID LIMIT
PL =PLASTIC LIMIT
NMC =NATURAL MOISTURE CONTENT
PSD =PARTICLE SIZE DISTRIBUTION
SG =SPECIFIC GRAVITY
PI =PLASTICITY INDEX
C =COHESION KN/M^2
Ø =ANGLE OF INTERNAL FRICTION
▽ =STATIC GROUND WATER LEVEL

DISTURBED SAMPLE
UNDISTURBED SAMPLE

REMARK :

LOGGED BY:
DATE:
APPROVED BY:
SCALE:

Borehole Data Collection Format for Foundation Investigation

CORE/GE/RF/086/B

CORE Consulting Engineers Plc
Tel: 251-11-3-206032,251-11-3-727013
Fax: 251-1-2306033 P.O.Box
Email: coreconsult@ethionet.et
Addis Ababa, Ethiopia

BOREHOLE LOG

BH No: 169

SHEET: 1 of 1

PROJECT: Addis Ababa Condominium buildings
CLIENT: Addis Ababa housing Construction Project Office
ITE LOCATION: Yeka-Tafo (BH-169)
BH COORDINATE(UTM-Adindan Datum)
EASTING: 487624
NORTHING: 997828
GROUND ELEVATION(m): 2100

DRILLING TYPE: Rotary drilling
INCLINATION: Vertical
TOTAL DEPTH DRILLED: 11.00m
GWL: not encountered
FLUSHING SYSTEM:
DATE STARTED: 31/10/15
DATE COMPLETED: 31/10/15

Depth (m)	Run Length	TCR	RQD	Hole dia.	Casing	Sampling	SPT	GW	Graphic Log	Field Description of Soil/Rock	Photo
0–1	1.5	55		108			3/3/4			firm, black, highly plastic silty clay	
1.5										1.5	
1.5–3	1.5	100				U	4/5/6			Whitish gray, stiff, highly plastic silty clay	
3–4	1	100									
4–5	1	100				U	8/16/18				
5										5	
5–7	1.5	100					10/12/14			Light grayish brown, very stiff, highly plastic Silty clay	
7										7	
7–9	1	0		89						Light brown, loose, moderately plastic, silty clay	
8–9	1.5	0					6/9/15				
9–11	2	0									
11										11	

BH = Borehole
N = Blows/30cm
SPT = Standatd Penetration test
USCS = Unified Soil Classifcation System

RQD = Rock Quality Designation
TCR = Total Core Recovery
GWL = Ground Water Level

D Distrubed Sample
U Undistrubed Sample
R Rock Sample

REMARK: sample not recovered from 7 up 11m, loose material

LOGED BY: _____
APPROVED BY: _____
SCALE: _____